STEM CELLS AND DEVELOPMENT
Volume 22, Number 3, 2013

DOI: 10.1089/scd.2012.0279

A Focused Microarray for Screening Rat Embryonic Stem Cell Lines

James Hong,[1] Hong He,[1] Phuoc Bui,[1] Ben Ryba-White,[1] Mohammad A.K. Rumi,[2] Michael J. Soares,[2] Debasree Dutta,[2,*] Soumen Paul,[2] Masaki Kawamata,[3] Takahiro Ochiya,[3] Qi-Long Ying,[4] Pavan Rajanahalli,[1] and Mark L. Weiss[1,5]

Here, we describe a focused microarray for screening rat embryonic stem cells (ESCs) and provide validation data that this array can distinguish undifferentiated rat ESCs from rat trophoblast stem (TS) cells, rat extraembryonic endoderm cells, mouse embryonic fibroblast feeder cells, and differentiated rat ESCs. Using this tool, genuine rat ESC lines, which have been expanded in a conventional rat ESC medium containing two inhibitors (2i), for example, glycogen synthase kinase 3 (GSK3) and mitogen-activated protein kinase (MEK) inhibitors, and leukemia inhibitory factor, and genuine rat ESCs, which have been expanded in rat ESC medium containing four inhibitors (4i), for example, GSK3, MEK, Alk5, and Rho-associated kinase inhibitors were compared; as were genuine rat ESCs from 4 different strains of rats. Expression of *Cdx2*, a gene associated with trophoblast determination, was observed in genuine, undifferentiated rat ESCs from 4 strains and from both 2i and 4i ESC derivation medium. This finding is in contrast to undifferentiated mouse ESCs that do not express *Cdx2*. The rat ESC focused microarray described in this report has utility for rapid screening of rat ESCs. This tool will enable optimization of culture conditions in the future.

Introduction

THE RAT LAGS BEHIND THE MOUSE in the field of functional genomics [1,2]. After 2 decades of trying, genuine rat embryonic stem cells (ESCs) were produced [3,4]. Recently, genuine rat ESCs were used to produce a knockout rat [5]. Several lines of evidence support the contention that the mechanism of self-renewal and maintenance of the ground state of pluripotency is fundamentally different in mice and humans. The differences that exist between human and rat ESCs or between rat and mouse ESCs are yet to be fully elucidated. For example, we recently reported that rat ESCs maintained using the 2 inhibitor cocktail of PD0325901, a mitogen-activated protein kinase (MEK) inhibitor, and CHIR99021, a glycogen synthase kinase 3 (GSK3) inhibitor plus leukemia inhibitory factor (LIF), called two inhibitors (2i) below, express *Cdx2* [6], a gene involved in trophoblast fate determination [7,8]. This finding is in sharp contrast to what is observed in mouse ESCs. Another difference is that rat ESCs cannot be maintained in medium containing only LIF when grown on inactivated mouse embryonic fibroblasts (MEFs), in contrast to mouse ESCs [9]. Finally, as reported for the mouse, strain differences may affect the quality of rat ESCs for producing germline transmission, or may affect the ability of the blastocyst to integrate ESCs and the efficiency of rat ESCs to contribute to the germline is lower than the mouse [3,4,6,10]. Therefore, distinct species differences exist between rat and mouse ESCs. Further work is needed to fully understand the differences between rat and mouse ESCs and to optimize rat ESC culture conditions to increase germline transmission efficiency.

Here, our goal was to develop and validate a rat-specific microarray focused on detection of pluripotency, stem cell and differentiation-associated gene expression for rapidly screening rat ESC lines, and enable the optimization of rat ESC culture. To derive this array, we culled the literature to generate a short list of genes that would discriminate undifferentiated and differentiated ESCs [11,12], and ESCs from extraembryonic endoderm cells (XEN, [13–15]), epiblast stem cells (Epi, [16–18]), and from trophoblast stem (TS) cells [19,20]. The gene list was provided to Qiagen and they manufactured the gene array. Next, we used this array to

[1]Department of Anatomy and Physiology, Kansas State University College of Veterinary Medicine, Manhattan, Kansas.
[2]Department of Pathology and Laboratory Medicine, University of Kansas Medical Center, Kansas City, Kansas.
[3]Division of Molecular and Cellular Medicine, National Cancer Center Research Institute, Tokyo, Japan.
[4]Department of Cell and Neurobiology, Keck School of Medicine, University of Southern California, Los Angeles, California.
[5]The Midwest Institute of Comparative Stem Cell Biology, Kansas State University, Manhattan, Kansas.
*Present affiliation: Rajiv Gandhi Centre for Biotechnology, Thiruvananthapuram, India.

compare the gene expression of genuine rat ESCs produced in our laboratory [6] and from the laboratory of QY [4] using 2i medium and genuine ESCs produced using media containing four inhibitors (4i, the Rho-associated kinase inhibitor Y-27632; the MEK inhibitor PD0325901; the type 1 TGFβ receptor inhibitor A-83-01; and the GSK inhibitor CHIR99021, called 4i below [10]. The 4i genuine rat ESCs were provided by the laboratory of MK and TO. The data show that the array has sensitive quality assurance and quality control elements, good inter-investigator reliability, and good reproducibility between different genuine rat ESC lines. These data confirm that genuine rat ESCs express *Cdx2* since genuine rat ESCs from 3 different labs express the gene with rat ESCs expanded in YPAC medium expressing *Cdx2* at the highest levels. In conclusion, this array discriminates undifferentiated rat ESCs from differentiated rat ESCs and discriminate ESCs from extraembryonic endoderm stem cells (XEN) and TS cells, as well as, other stem cells derived from the developing rat embryo. Therefore, this array is a sensitive, validated tool for rapidly screening rat ESCs lines and for optimizing rat ESC culture conditions.

Materials and Methods

Cell lines

Information about samples and sample processing is listed in Table 1. Rat ESC lines used here were derived from Dark Agouti (DA) and transgenic Fischer 344 (F344) rats. ESC derivation, ESC differentiation to embryoid bodies (EBs), and characterization of our DA and F344 ESCs was described previously [6]. In addition, 2i plus LIF genuine rat ESC pellets derived from DA rats were provided by Dr. Q. Ying (University of Southern California, Los Angeles, CA) [4]. Genuine rat ESC pellets derived from Long Evans Agouti and Wistar rats using the 4i medium were provided by Drs. M. Kawamata and T. Ochiya (National Cancer Center Research Institute, Tokyo, Japan) [10]. Rat TS and extraembryonic endoderm stem cells (XEN) were prepared as previously described and were provided by Drs. M. Rumi and M. Soares [19,21]. Mitotically inactivated CF-1 MEFs (passage 3) were obtained and used following the manufacturer's protocol (Globalstem).

Reverse transcriptase–polymerase chain reaction focused array

The gene list and efficiency data and sample processing is listed in Table 1. The 96-well custom array containing 92 unique elements for evaluation of rat ESCs was manufactured by Qiagen (CAPR10083). We did not independently validate the manufacturer's PCR efficiency assays for each gene. Total RNA was prepared using the RNeasy RNA isolation kit (Qiagen) or TRIZOL (Life Technologies) using the manufacturer's protocol. Complementary DNA was synthesized using Qiagen's RT^2 first strand kit following the

Table 1. Biological Samples

Sample number	*Sample name*	*Total RNA preparation*	*Source*
Sample 1 & 2	XEN	TRIZOL	Provided by Michael Soares' lab University of Kansas Medical Center
Sample 3 & 4	inactivated MEF	Rneasy RNA isolation kit (qiagen) per manufacturer's protocol	Purchased from GlobalStem
Sample 5 & 6	DA54.1 p9 chimera	Rneasy RNA isolation kit (qiagen) per manufacturer's protocol	Generated in house as described in Hong et al. [6]
Sample 7 & 8	Fischer 344 2.1.1 p24, unknown	Rneasy RNA isolation kit (qiagen) per manufacturer's protocol	Generated in house as described in Hong et al. [6]
Sample 9 & 10	DA52 p9, GERMLINE	Rneasy RNA isolation kit (qiagen) per manufacturer's protocol	Generated in house as described in Hong et al. [6]
Sample 11 & 12	DAc8, p35, GERMLINE	Rneasy RNA isolation kit (qiagen) per manufacturer's protocol	Provided by Qilong Ying's lab University of Southern California, generated per Li et al. [4]
Sample 13 & 14	DA54.1 EB, 5 d	Rneasy RNA isolation kit (qiagen) per manufacturer's protocol	Generated in house as described in Hong et al. [6]
Sample 15 & 16	DA54.1 EB, 10d	Rneasy RNA isolation kit (qiagen) per manufacturer's protocol	Generated in house as described in Hong et al. [6]
Sample 18 & 19	TS	TRIZOL per manufacturer's protocol	Provided by Michael Soares' lab University of Kansas Medical Center
Sample 19 & 20	DA53.1, p10, GERMLINE	Rneasy RNA isolation kit (qiagen) per manufacturer's protocol	Generated in house as described in Hong et al. [6]
Sample 25 & 26	Fischer 344 38, GERMLINE	Rneasy RNA isolation kit (qiagen) per manufacturer's protocol	Generated in house as described in Hong et al. [6]
Sample 31 & 32	115 LEA, p6, 4i	Rneasy RNA isolation kit (qiagen) per manufacturer's protocol	Provided by Kawamata and Ochiya [10], National Cancer Center Research Institute, Tokoyo, Japan
Sample 33 & 34	116 Wistar, p5, 4i	Rneasy RNA isolation kit (qiagen) per manufacturer's protocol	Provided by Kawamata and Ochiya [10], National Cancer Center Research Institute, Tokoyo, Japan

manufacturer's protocol. The focused array was run using Qiagen's RT^2 qPCR MasterMix for the BioRad iQ5 thermal cycler. Thermal cycling and quantitation were performed using a BioRad iQ5 iCycler controlled by Biorad iCycler IQ software version 3.1.7050. Following PCR, the products were subjected to melting point analysis. All biological samples were run in duplicate (technical replicates) independently prepared by different investigators (JH or HH). The array data were uploaded to the gene expression omnibus (GEO) website (www.ncbi.nlm.nih.gov/geo, Accession number GSE30582).

Reverse transcriptase–polymerase chain reaction to test for rat genomic DNA contamination

Total RNA samples used in the array were tested for rat genomic DNA contamination (RGDC). Complementary DNA was synthesized using Superscript III First-Strand Synthesis Supermix kit (Life Technologies) primed with oligo-dT_{12-18} per the manufacturer's protocol. A primer set for rat PBGD was designed that spanned an intron and was validated to discriminate genomic DNA (primer sequence available upon request). PCR was performed using a BioRad iCycler or iQ5: the initial denaturation at 95°C for 3 min, 30 cycles of (94°C for 30 s, 53°C–55°C for 30 s, and 72°C for 1 min), and the final extension at 72°C for 10 min. Following PCR, the products were resolved on a 1% agarose gel with 100 bp DNA ladder (Promega) and imaged.

Data analysis and assembly of figures

No calls or missing data were assigned Ct value of 40.0. Data were loaded into Microsoft Excel 2010 for analysis (raw and transformed data are in Supplementary Table S1; Supplementary Data are available online at www.liebertpub.com/scd). The average threshold cycle (Ct), standard deviation, and % covariance were calculated for selection of housekeeping gene (HKG) candidates. Unmanipulated data from technical replicates were plotted in a scattergram and a linear regression line was calculated using SigmaPlot version 12. To evaluate the impact of normalizing the data using HKG, the 5 experimental genes with the lowest standard deviations were inspected using the RefFinder tools available via the Cotton EST database (www.leonxie.com/referencegene.php) that facilitates comparison of HKG using major computational programs such as geNorm [22], Normfinder [23], BestKeeper [24], and the comparative Ct method [25]. Two of these genes (*Gapdh* and *Ldha*) were used to normalize the Ct data and the scattergrams were plotted and linear regression lines and R^2 values calculated (see Results section). For simplicity of calculation, we assumed 100% PCR replication efficiency and used $2^{(-\Delta\Delta Ct)}$ to calculate fold change. We did this despite knowing the manufacturer's quality assurance and quality control (QA/QC) specifications PCR efficiency data for each gene in the array (Table 1) because we assumed that experimental amplification efficiency might differ. Kruskal–Wallis Analysis of Variance for Ranks was used to determine overall differences between biological samples. Following significant ANOVA, Student-Newman–Keuls test was used for post hoc testing of planned comparisons. Unless specified differently, 10 or 100-fold increases or decreases in gene expression were selected as critical values for significant differences in gene expression between groups. Significance was set at $\alpha < 0.05$.

Results

QA and QC

SABioscience/Qiagen RT^2 profiler array has 7 wells dedicated to QA and QC.

(1) RGDC QA/QC step. RGDC is a concern since it can affect the interpretation of array findings. To obviate this potential problem, we used DNaseH treatment during isolation of total RNA in some samples. For every sample, SuperArray's RT^2 First Strand Kit (Qiagen) was used with its genomic DNA elimination step. RGDC was evaluated by calculating Ct of the RGDC–Ct HKG. RGDC was considered questionable if the difference was <14. Using this criterion, 2 samples [one replicate of Ying ESCs (DAc8) and one replicate of TS cells] had questionable results as to RGDC. To investigate those cases, RGDC was evaluated using reverse transcriptase–polymerase chain reaction (RT-PCR) using a primer set that spans an intron and the amplicon run on a 1% agarose gel along with a rat genomic DNA positive control. As shown in Fig. 1A, RGDC was not confirmed by RT-PCR. The fact that the technical replicate did not flag RGDC and that the RT-PCR did not confirm RGDC in these 2 cases suggest that the RGDC test reported a false positive 2 times in 26 arrays (about 8% error rate).

(2) Reverse transcriptase efficiency (RTE) QC step. RTE can be impacted by poor RNA quality or contaminants in the sample. RTE was evaluated by calculating average Ct of the reverse transcriptase control (RTC)–average Ct of the positive PCR control (PPC) from the triplicate wells on the array. The manufacturer's specification was that the difference should be <5. All samples passed (average 3.9 ± 0.42, range = 3.3–4.5).

(3) PCR amplification efficiency QC step. PCR efficiency should be consistent across arrays to reduce the need of making many technical replicates to achieve consistent, reproducible data. PCR efficiency was evaluated by calculating the average Ct of the triplicate PPC wells in the array. The manufacturer's specifications state that the PPC Ct values should be an average of 20 ± 2 cycles across in an experiment. We observed an average of 19.5 ± 0.2, meeting the PCR efficiency specification. In addition, the manufacturer has designed the PCR primers and tested their efficiency. The average efficiency of the primers in this array was $108.4\% \pm 10.1\%$ (range 90.5%–146.8%). Primer efficiency information provided by Qiagen is found in Table 1.

(4) Production of a single PCR product QA/QC step. Following amplification, the products were subjected to a melting point analysis to confirm that a single product was produced. Based upon the melting point analysis, PCR produced a single product in every case (data not shown).

Selection of the HKG and evaluation of technical replicates

To select the HKG, the standard deviation of Ct values for each gene in the array was sorted from lowest to highest (see Supplementary Table S1). Of the experimental genes, *Actb*, *Ctnnbl1*, *Ldha*, *Hdac2*, and *Gapdh* had the lowest standard deviations (0.72, 0.73, 0.78, 0.82, and 1.06, respectively). Next, we compared the effect of normalization on the regression R^2 values between 9 biologically independent pairs of technical replicates and compared the R^2 of raw Ct values and the R^2

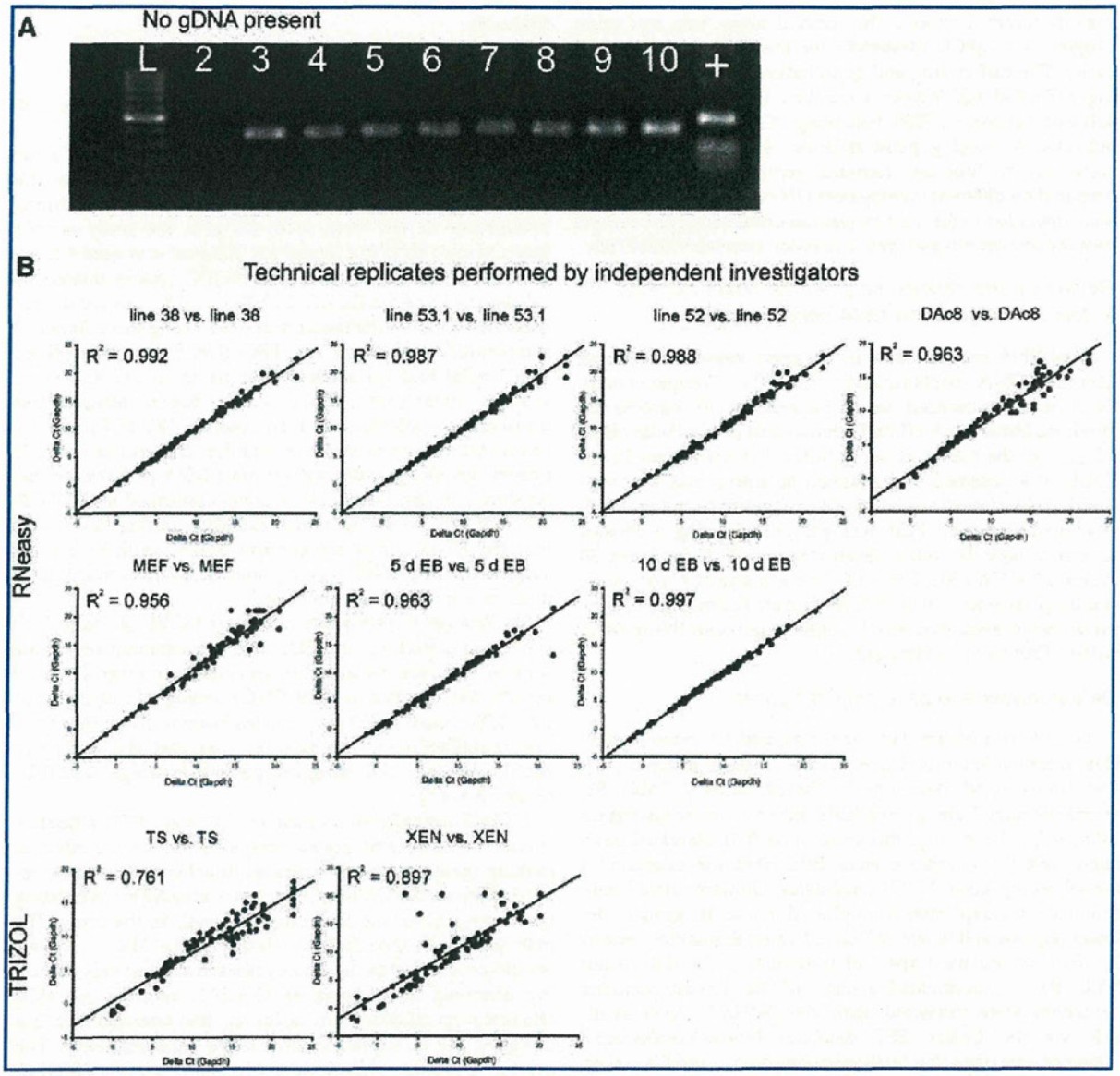

FIG. 1. **(A)** Evaluation of rat genomic DNA contamination (RGDC). Reverse transcriptase–polymerase chain reaction (RT-PCR) was performed using a primer pair that spans an intron to evaluate whether RGDC was present. No evidence of RGDC was found, indicating that the array RGDC well provided false positive in 2 instances (2 out of 18 arrays). Lane 2 is RNA sample prepared from inactivated mouse embryonic fibroblasts (MEFs). Lane 3 is RNA sample from undifferentiated genuine rat embryonic stem cells (ESCs). Lane 4 is RNA sample prepared from rat extraembryonic endoderm (XEN) cells. Lanes 5–7 are RNA samples from 3 different ESC lines prepared in-house [Dark Agouti (DA) line 1 (line 53.1), Fischer 344 (line 38), DA line 2 (line 52), respectively]. Lane 8 is an RNA sample prepared from rat trophoblast stem (TS) cells. Lanes 9 and 10 are RNA samples prepared from DA ESCs differentiated to 5 day embryoid bodies (EBs, lane 9) and 10 day EBs (lane 10). A rat genomic DNA sample positive control is labeled "+" (amplicon at 354 bp for cDNA and 433 bp for genomic DNA). Lane 1 (L) is a standard 100 bp ladder. **(B)** Comparison of technical replicates performed by independent investigators using scattergram and regression line with the R^2 value. *Top panel* is RNA samples isolated using the RNeasy kit (RNeasy). *Bottom panel* is RNA samples isolated using the TRIZOL method (TRIZOL). Note that the RNeasy isolation kit produced consistently higher R^2 values than the TRIZOL method. Scattergrams of ΔCt values (*Gapdh* used to normalize data).

after normalization with *Ldha* and *Gapdh*. There was no significant difference between the R^2 values of technical replicates not normalized and those normalized using *Ldha* or *Gapdh* (no normalization $R^2 = 0.940 \pm 0.083$, range = 0.735–0.997; *Gapdh* normalized $R^2 = 0.945 \pm 0.074$, range 0.761–0.994; and *Ldha* normalized $R^2 = 0.945 \pm 0.074$, range 0.761–0.994). Using the tools found at the Cotton EST database (see Methods section), *Gapdh* and *Ldha* were selected as the HKG. The geometric mean of *Gapdh* and *Ldha* was used as HKG for normalization (see Supplementary Table S1).

As shown in Fig. 1B, based upon the R^2 values cited above, the technical replicates performed by different investigators showed good reproducibility across 9 biological samples evaluated. We observed that total RNA sample preparation using the RNeasy column method tended to produce tighter reproducibility than the TRIZOL method (TS and XEN samples were prepared using the TRIZOL method).

The array can discriminate undifferentiated rat ESCs from differentiated ESCs, XEN, TS, and MEFs

As shown on the top of Fig. 2, when overall gene expression of 3 genuine undifferentiated rat ESC samples expanded in 2i plus LIF from the Weiss lab (lines 52 and 53.1

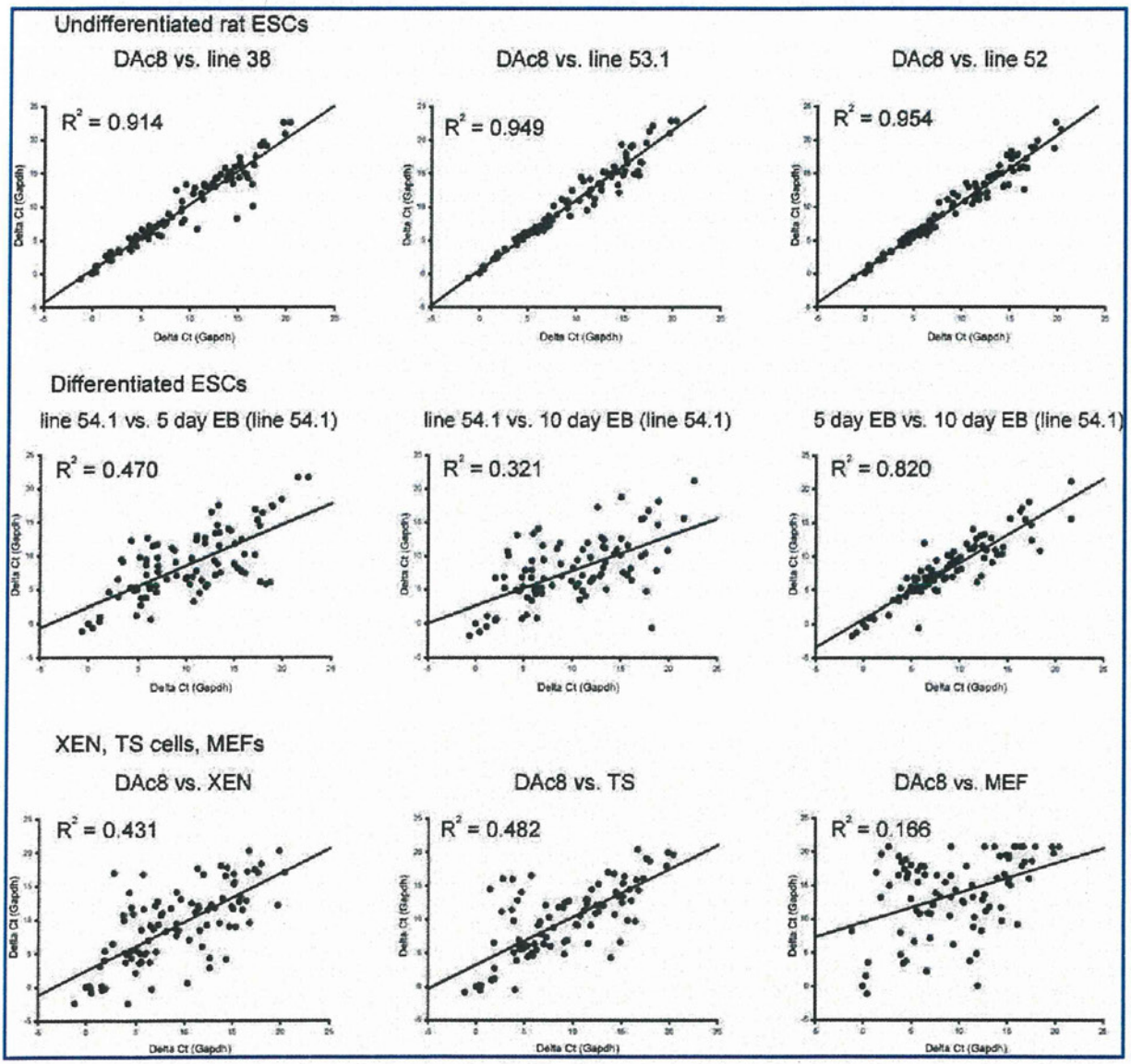

FIG. 2. Comparison of biological samples using scattergram and regression line with the R^2 value. *Top panel:* Rat ESC lines derived in-house (DA ESC lines 53.1 and 52 and transgenic Fischer 344 ESC line 38) compared with QY's genuine rat ESCs (DAc8). Statistically, there are no significant differences between overall gene expression patterns of the ESC lines. There was a trend for genuine DAc8 versus DA lines 53.1 and 52 to have higher coherence (R^2 values > 0.949) than genuine DAc8 versus F344 line 38 (R^2 value = 0.914). *Center panel:* (*left and middle graphs*) Comparison of the undifferentiated parental DA ESC cell line (line 54.1) with the 5 day and 10 day differentiated EBs derived from line 54.1. (*Right graph*) Comparison of 5 day and 10 day differentiated EBs. Note that statistical testing revealed that the undifferentiated DA line 1 (line 54.1) was significantly different from the same ESC line after 10 day EB formation (*middle graph*) and that gene expression by 5 day EBs was significantly different from 10 day EBs (*right graph*). *Bottom panel:* Comparison of DAc8 genuine rat ESCs to cells from the XEN, *left graph*; TS cells, *middle graph*; and inactivated MEFs, *right graph*]. By inspection, one can observe differences in gene expression between ESCs and non-ESC cell lines based upon y-intercept (expected to be zero in similar lines), scatter about the regression line and R^2 values < 0.5.

from DA rats and line 38 derived from transgenic F344 rats) were compared with undifferentiated genuine rat ESCs expanded in 2i plus LIF from QY's lab (derived from DA rats, line DAc8), there was good coherence in terms of gene expression as indicated by R^2 values >0.91. There was a tendency for higher correlations between undifferentiated DA (DAc8) versus DA ESC lines 53.1 and 52 (Fig. 2, top panel middle and right) when compared with DA versus F344 line 38 (Fig. 2, top panel left).

To statistically evaluate the samples, a Kruskal–Wallis One-Way Analysis on Ranks was used, which indicated overall significant differences between the 8 biological samples. Next, Student-Newman–Keuls method was used for planned multiple comparisons, and no significant differences were found between the 4 independently derived 2i plus LIF genuine rat ESC samples. In contrast, multiple comparisons revealed a significant difference between the undifferentiated ESC line and the same cells after 10 days of differentiation to EBs, which is supported by the observation of poor correlation between undifferentiated and differentiated samples (Fig. 2, middle panel). As shown in Fig. 2 bottom panel, the overall gene expression patterns shown in the scattergrams for undifferentiated ESCs poorly correlated with rat XEN, rat TS, and inactivated MEFs, too. These suggest differences in gene expression between undifferentiated ESCs and the other cell types.

To evaluate differences in gene expression between cell types, 10-fold and 100-fold differences in expression were selected as arbitrary thresholds. When inactivated MEFs were compared with undifferentiated ESCs (both those derived in 2i plus LIF and those derived in 4i), 47 genes were expressed at >10-fold higher levels in undifferentiated ESCs and 8 genes were found to be expressed at >10-fold higher levels in MEFs (see Supplementary Table S2). Further, 24 genes were expressed at >100-fold higher levels in undifferentiated ESCs and 2 genes were expressed at >100-fold higher levels in MEFs (see Fig. 3A). Notably, genes *Stella*, *Utf1*, *Pou5f1* (*Oct4*), *Gdf3*,*Bex1*, and *Pecam1* were expressed at very high levels in ESCs, about 161666–9717-fold higher levels and the genes *Ptn and Inhba* were expressed 1556-123-fold higher levels in MEFs (see Fig. 3A).

Comparison of undifferentiated ESCs with differentiated ESCs. When gene expression of undifferentiated ESCs was compared with gene expression after 5 days differentiation to EBs, 33 genes had greater than 10-fold expression differences between the 2 groups, and 10 genes were expressed higher in undifferentiated ESCs and 23 genes were expressed >10-fold higher levels in EBs after 5 days of differentiation (see Supplementary Table S3). Twelve genes showed >100-fold differences in gene expression between undifferentiated ESCs and EBs after 5 days of differentiation. As shown in Fig. 3B (left), genes *Gdf3* and *Tcl1a* were expressed at >100-fold higher levels in undifferentiated ESCs (range 243- to 134-fold higher) and the genes *Cer1*, *Afp*, *Actc1*, *Foxa2*, *Gata4*, *Gata6*, *Hand1*, *Sox7*, *Sox17*, and *Pdx1* were expressed >100-fold higher levels in the 5 day differentiated ESCs (range of 18183- to134-fold higher). When gene expression of undifferentiated ESCs was compared with gene expression after 10 day differentiation to EBs, 45 genes had >10-fold expression differences between groups (see Supplementary Table S3). Ten genes were expressed at >10-fold higher levels in undifferentiated ESCs and 35 genes were expressed at >10-fold higher levels in EB differentiated for 10 days. Figure 3B (right) shows the 19 genes that had >100-fold expression difference between these groups. Note that the genes *Gdf3*, *Fgf4*, *Tcl1a*, *Nanog*, and *Stella* were expressed >100-fold in undifferentiated ESCs (range of 416–109-fold higher) and the genes *Afp*, *Cer1*, *Actc1*, *Foxa2*, *Hand1*, *beta-globin*, *Gata4*, *Sox7*, *Gata6*, *Pitx2*, *Pdx1*, *Prdm1*, *Kdr*, and *Gata5* were expressed at >100-fold higher levels in EBs after 10

FIG. 3. Differences in gene expression detected by the array. **(A)** List of genes that showed >100-fold expression differences between undifferentiated ESCs [all undifferentiated ESCs: both two inhibitors (2i) plus LIF and four inhibitors (4i) ESCs included] and inactivated MEFs. On the *left*, genes that were highly expressed in ESCs are shown in descending order. On the *right*, genes that were highly expressed in MEFs. For a complete, ordered list, see Supplementary Table S1. **(B)** Effect of differentiation for 5 or 10 days on gene expression. **(B)** *Left:* List of genes that showed >100-fold expression differences between undifferentiated ESCs (all undifferentiated ESCs: both 2i plus LIF and 4i ESCs included) versus 5 days of differentiation. Two genes that are highly expressed in undifferentiated ESCs are shown on the *left*, and 10 genes that were expressed by differentiation are listed on the *right*. **(B)** *Right:* List of genes that showed >100-fold expression differences between undifferentiated ESCs (all undifferentiated ESCs: both 2i plus LIF and 4i ESCs included) versus 10 days of differentiation. Five genes that are highly expressed in undifferentiated ESCs are shown on the *left*, and 14 genes that were expressed by differentiation are listed on the *right*. For a complete, ordered list, see Supplementary Table S2. **(C)** Comparison of undifferentiated ESCs with other cells derived from rat embryos. **(C)** *Left:* List of genes that showed >100-fold expression differences between undifferentiated ESCs (all undifferentiated ESCs: both 2i plus LIF and 4i ESCs included) versus XEN cells. Seven genes that were more highly expressed in ESCs are shown on the *left* and 5 genes that were more highly expressed in XEN cells are shown on the *right*. For a complete, ordered list, see Supplementary Table S3. **(C)** *Right:* List of genes that showed >100-fold expression differences between undifferentiated ESCs (all undifferentiated ESCs: both 2i plus LIF and 4i ESCs included) versus TS cells. Eight genes that were more highly expressed in ESCs are shown on the *left*, and one gene, *Hand1*, which was highly expressed in TS cells is shown on the *right*. For a complete, ordered list, see Supplementary Table S4. **(D)** Comparison of derivation methods and comparison of 2i germline versus 2i chimera ESC lines. **(D)** *Left:* List of genes that showed >10-fold expression differences between undifferentiated ESCs derived and expanded in 2i plus leukemia inhibitory factor (LIF) conditions (2i ESCs) and ESCs derived and expanded in YPAC conditions (4i ESCs). On the *left*, note that one gene, Rpl13a was more highly expressed in 2i ESCs. On the *right*, 10 genes were more highly expressed in 4i ESCs, including Actc1, which was expressed 174-fold higher. For a complete, ordered list, see Supplementary Table S5. **(D)** *Right:* List of genes that showed >3-fold expression differences between undifferentiated 2i ESCs that contribute to the germline (Germline 2i ESCs) and undifferentiated 2i ESCs that contribute to chimera only (2i chimera ESCs). On the *left* is listed 6 genes that were more highly expressed in Germline 2i ESCs. On the *right* are listed 5 genes that were more highly expressed in Chimera 2i ESCs. For a complete, ordered list, see Supplementary Table S6.

days of differentiation (range 337663- to 114-fold higher). Thus, as ESCs undergo differentiation over time, more lineage specification and lineage specific genes are expressed in EBs, as one would expect.

Comparison of undifferentiated ESCs with XEN cells. As one might expect from inspection of Fig. 2 (bottom), 34 genes showed > 10-fold expression differences between undifferentiated rat ESCs and XEN cells, and 18 genes were expressed > 10-fold higher in undifferentiated ESCs and 24 genes were expressed at > 10-fold higher levels in XEN cells (see Supplementary Table S4). As shown in Fig. 3C (left), genes *Nanog*, *Fgf4*, *Sox2*, *Klf4*,*Isl1*, *Ptn*, and *Nodal* showed > 100-fold higher expression in undifferentiated ESCs (range of 19924- to 101-fold higher). In contrast, the genes *Gata6*, *Gata4*, *Pdgfra*, *Sox17*, and *Lamb1* were expressed at 100-fold higher levels in XEN cells (range 1249- to 115 times higher expression).

Comparison of undifferentiated ESCs with TS cells. Twenty-four genes showed > 10-fold expression difference between undifferentiated rat ESCs and TS cells. Of these 24 genes, 16 genes were expressed > 10-fold higher in undifferentiated ESCs and 8 genes showed > 10-fold higher expression in XEN

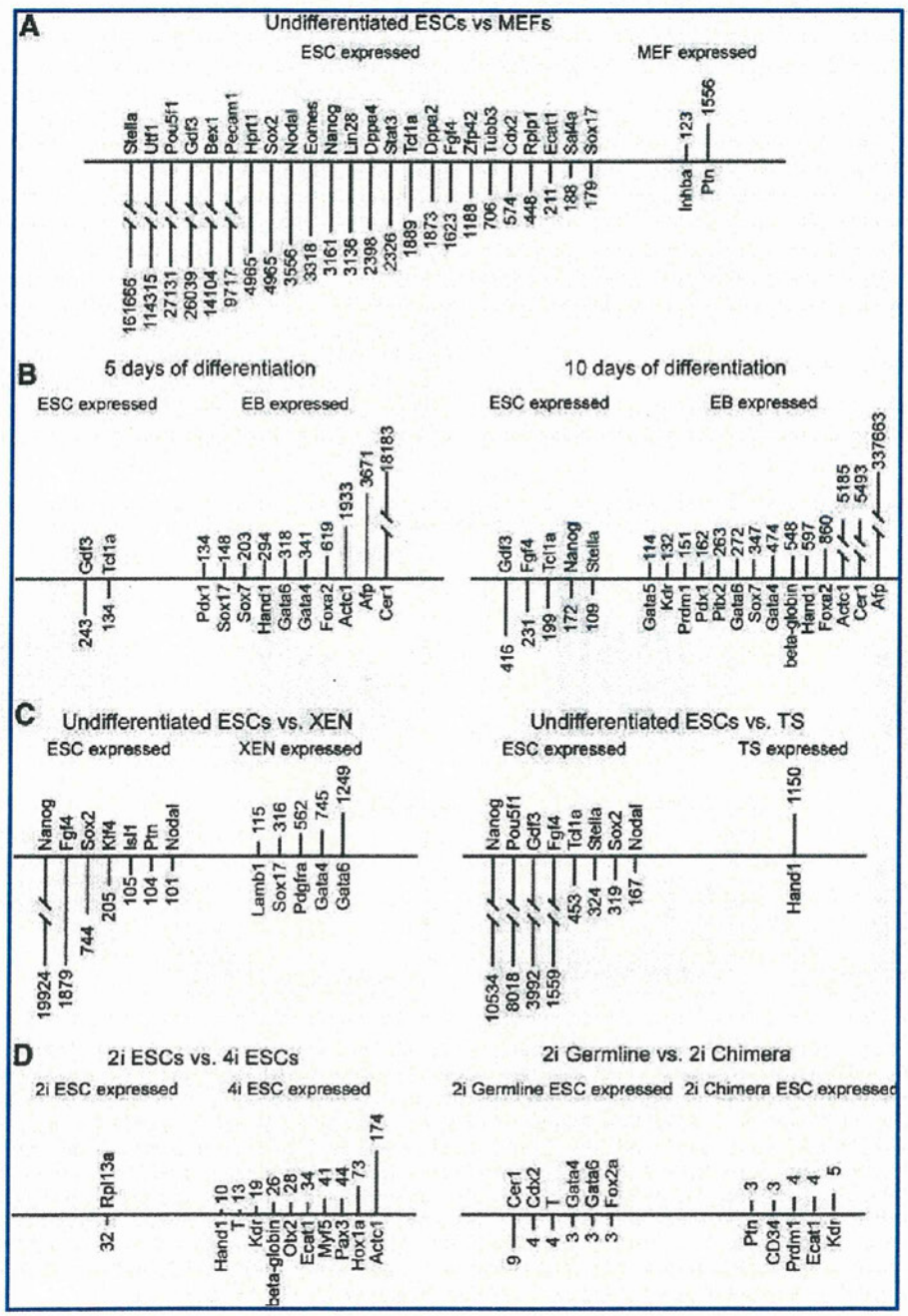

(see Supplementary Table S5). As shown in Fig. 3C (right), *Nanog*, *Pou5f1* (*Oct4*), *Gdf3*, *Fgf4*, *Tcl1a*, *Stella*, *Sox2*, and *Nodal* were expressed at > 100-fold higher levels in undifferentiated rat ESCs (ranging from 10534 to 167 times higher expression); *Hand1* was expressed at > 100-fold higher levels in TS cells (1150 times higher expression).

Comparison of 2i plus LIF with 4i derivation methods. When germline ESCs derived in 2i plus LIF were compared with germline ESCs derived in 4i, 12 genes were found to exceed the > 10-fold difference in expression threshold, and only one gene was found to have > 100-fold difference in expression (see Supplementary Table S6). As shown in Fig. 3D (left), the gene *Rpl13a* was expressed 32-fold higher levels in 2i plus LIF germline ESCs and the genes *Actc1*, *Hox1a*, *Pax3*, *Myf5*, *Ecat1*, *Otx2*, *beta-globin*, *Kdr*, *T*, and *Hand1* were expressed at higher levels in 4i ESCs (range of 174- to 10-fold higher, respectively).

Comparison of germline to chimera ESCs. When germline ESC derived in 2i plus LIF were compared with ESCs derived in 2i plus LIF that only formed chimera, no genes were found to meet the criteria levels of > 10-fold difference in gene expression (see Supplementary Table S7). As shown in Fig. 3D (right), in germline 2i plus LIF ESCs, the gene *Cer1* was found to be expressed at 9-fold higher level. In chimera ESCs, *Kdr* was found to be expressed at 5-fold higher levels.

Gene expression of selected genes

As shown in Fig. 4, when the fold expression was calculated and normalized using *Ldha* and *Gapdh* as HKG and MEFs as the control cell using the $2^{-\Delta\Delta Ct}$ method, undifferentiated rats ESCs expressed the transcription factors *Gdf3*, *Nanog*, *Pou5f1* (*Oct4*), and *Sox2* at relatively high levels and these clearly distinguish undifferentiated ESCs from the other groups. As we reported [6], *Cdx2* is expressed by undifferentiated rat ESCs (see Fig. 4, bottom left). Here, we noted that genuine rat ESCs expanded in 2i plus LIF express *Cdx2* at a lower level than TS cells. In contrast, genuine rat ESCs expanded in 4i medium (YPAC) express *Cdx2* at > 3-fold higher level than rat ESCs expanded in 2i plus LIF and at a higher level than rat TS cells. Thus, a tremendous variability in *Cdx2* expression was observed in genuine rat ESCs. It is also noted that differentiation of rat ESCs that were grown in 2i plus LIF conditions to EBs resulted in an increase of *Cdx2* expression. This might suggest that rat ESCs may easily differentiate along the extraembryonic lineage. This notion is supported by the induction of *Hand1*, *Eomes* and, *Fgfr2* by EB formation (*Eomes* and *Ffg42* shown in Fig. 4).

The rat ESC array list. Prior to normalization of the gene array data, PPC and RTC had the lowest variation followed by experimental genes *Gapdh*, *Ldha*, *Hdac2*, *Ctnnbl1*, and *Actb* (see Table 2). As presented above, these genes were evaluated as potential HKG using the Cotton EST database RefFinder tools and *Gapdh* and *Ldha* were selected. As shown in the bottom of Table 2, following normalization using HKG and averaging of the technical replicates, the variation of *Gapdh* and *Ldha* was < PPC and RTC, as expected. It is interesting to note that after normalization, the variation of *Hdac2*, *Ctnnbl1*,and *Actb* was < PPC and RTC, too (see Supplementary Table S1). This suggests that these 5 genes cluster.

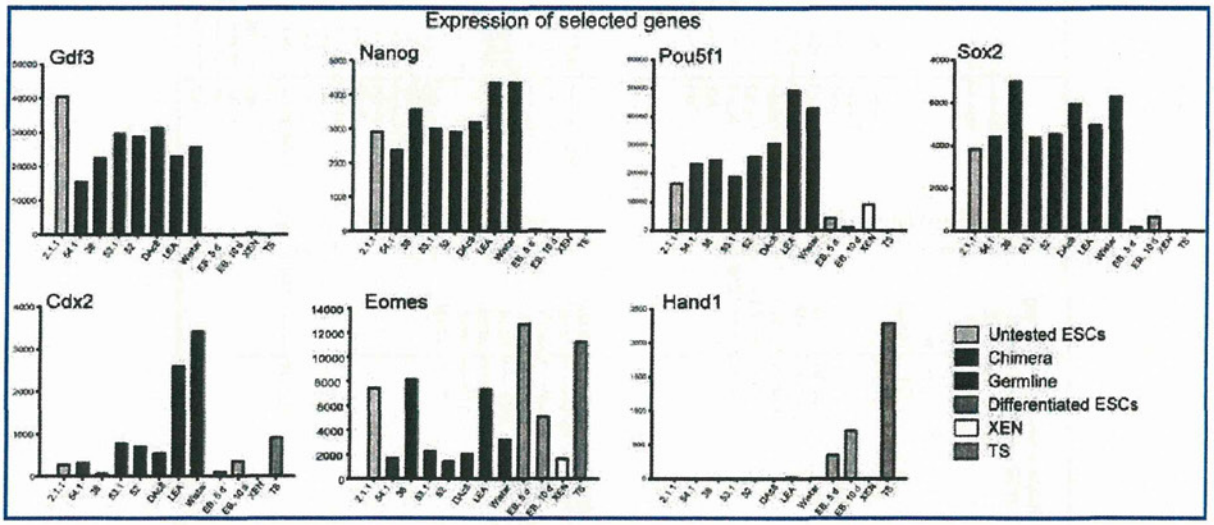

FIG. 4. Normalized expression of 7 genes by biological samples. Genes were selected based upon their ability to differentiate between the cell types, for example, undifferentiated rat ESCs, differentiated ESCs and XEN, and TS cells. Note that undifferentiated ESCs expressed the transcription factors *Gdf3*, *Nanog*, *Oct4* (*Pou5f1*), and *Sox2* at 1000-fold higher levels than differentiated ESCs or the XEN or TS cells. Note that the expression of these genes was decreased by differentiation of rat ESCs to EBs. Note that rat ESCs expressed markers of the trophoblast lineage, *Cdx2 and Eomes*, suggesting that rat ESCs may have a capacity to differentiate along this lineage. In support of this notion, differentiation of rat ESCs induces the expression of *Hand1*. Note that ESC derived from DA rats (lines 54.1, 53.1, 52, and DAc8), lines derived from F344 rats (line 2.1.1 and 38), and lines derived from Long Evans Agouti and Wistar (LEA and WIS), express the transcription factors *Gdf3*, *Nanog*, *Oct4* (*Pou5f1*), and *Sox2* at similar levels, and they express *Cdx2*, too. Note that all genuine ESCs: those ESCs derived and maintained in 2i plus LIF and ESCs derived and maintained in 4i conditions, express *Cdx2*; and that ESCs derived in 4i conditions express *Cdx2* at 3–4-fold higher levels than that ESCs derived in 2i plus LIF conditions.

TABLE 2. GENE LIST AND EFFICIENCY, PHYSICAL LAYOUT (WELL MAP)

No.	Position	Cat	Gene symbol	Refseq #	Official full name	Ct	E (%)	R
1	A1	PPR42970A	*Actc1*	NM_019183	Actin, alpha, cardiac muscle 1	24.56	106.8%	0.9995
2	A2	PPR44288A	*Afp*	NM_012493	Alpha-fetoprotein	23.75	112.7%	0.9996
3	A3	PPR06570A	*Actb*	NM_031144	Actin, beta	24.80	104.6%	0.9994
4	A4	PPR53512A	*Ctnnbl1*	NM_001024870	Catenin, beta-like 1	25.07	108.8%	0.9997
5	A5	PPR54901A	*LOC689064*	XM_001069372	Beta-globin	24.28	113.5%	0.9992
6	A6	PPR44291A	*Bex1*	NM_001037365	Brain expressed gene 1	23.32	111.9%	0.9993
7	A7	PPR57030A	*Prdm1*	XM_228320	PR domain-containing 1, with ZNF domain	24.79	104.7%	0.9998
8	A8	PPR06561A	*Bmp4*	NM_012827	Bone morphogenetic protein 4	24.87	101.9%	0.9996
9	A9	PPR59972A	*T*	XM_217890	T, brachyury homolog (mouse)	23.74	102.7%	0.9998
10	A10	PPR55773A	*Cd34*	XM_223083	CD34 molecule	23.85	102.3%	0.9999
11	A11	PPR51519A	*Cdx2*	NM_023963	Caudal type homeo box 2	23.88	109.1%	0.9995
12	A12	PPR66629A	*RGD1563046*	XR_008686	Similar to cerberus-like	24.79	146.8%	0.9989
13	B1	PPR45580A	*Myc*	NM_012603	Myelocytomatosis oncogene	24.14	107.2%	0.9991
14	B2	PPR68946A	*Dazl*	NM_001109414	Deleted in azoospermia-like	27.48	103.5%	1.0000
15	B3	PPR45645A	*Dkk3*	NM_138519	Dickkopf homolog 3 (Xenopus laevis)	25.74	109.9%	0.9995
16	B4	PPR42793A	*Mapk3*	NM_017347	Mitogen activated protein kinase 3	23.26	109.6%	0.9997
17	B5	PPR68945A	*Dppa2*	XM_001063497	Developmental pluripotency associated 2	24.81	135.4%	0.9985
18	B6	PPR68425A	*LOC685378*	XM_001063552	Similar to developmental pluripotency associated 4 isoform 1	21.84	109.4%	0.9997
19	B7	PPR47830A	*Pias1*	XM_217188, XM_001074210, NM_001106829	Protein inhibitor of activated STAT, 1	24.82	111.8%	0.9988
20	B8	PPR57113A	*Eomes*	XM_001061749	Eomesodermin homolog (Xenopus laevis)	25.03	117.4%	0.9975
21	B9	PPR66519A	*Ecat1*	XM_001053599	ES cell-associated transcript 1	25.53	113.4%	0.9995
22	B10	PPR55731A	*Cdcp1*	XM_236747	CUB domain-containing protein 1	24.11	112.1%	0.9998
23	B11	PPR59431A	*Esrrb*	NM_001008516	Estrogen-related receptor beta	25.91	90.9%	0.9992
24	B12	PPR47773A	*Fbxo15*	XM_341633	F-box protein 15	23.92	109.7%	0.9999
25	C1	PPR52297A	*Fgf4*	NM_053809	Fibroblast growth factor 4	23.99	134.5%	0.9990
26	C2	PPR06647A	*Fgf5*	NM_022211	Fibroblast growth factor 5	24.09	94.7%	0.9998
27	C3	PPR06654A	*Fgfr2*	XM_341940	Fibroblast growth factor receptor 2	26.19	101.4%	0.9999
28	C4	PPR45134A	*Foxa2*	NM_012743	Forkhead box A2	27.63	90.5%	0.9998
29	C5	PPR59440A	*Foxd3*	XM_575873	Forkhead box D3	25.14	93.3%	0.9992
30	C6	PPR48683A	*Gata2*	NM_033442	GATA-binding protein 2	25.02	91.4%	0.9976
31	C7	PPR48066A	*Gata4*	NM_144730	GATA-binding protein 4	26.00	91.4%	0.9997
32	C8	PPR66727A	*Gata5*	NM_001024316	GATA-binding protein 5	24.37	106.2%	0.9994
33	C9	PPR44170A	*Gata6*	NM_019185	GATA-binding protein 6	23.91	107.3%	1.0000
34	C10	PPR53058A	*Gbx2*	XM_346072	Gastrulation brain homeobox 2	23.82	108.9%	0.9996
35	C11	PPR50097A	*Nr6a1*	XM_342427	Nuclear receptor subfamily 6, group A, member 1	24.36	102.9%	1.0000
36	C12	PPR63353A	*Gdf3*	XM_575661	Growth differentiation factor 3	24.13	104.1%	0.9995
37	D1	PPR49194A	*Hand1*	NM_021592	Heart and neural crest derivatives expressed 1	23.84	115.6%	0.9998
38	D2	PPR42588A	*Hdac2*	XM_342149	Histone deacetylase 2	24.09	101.9%	1.0000
39	D3	PPR44530A	*Inhba*	NM_017128	Inhibin beta-A	24.49	98.6%	0.9993
40	D4	PPR48904A	*Isl1*	NM_017339	ISL LIM homeobox 1	24.39	111.4%	0.9999
41	D5	PPR06671A	*Kdr*	NM_013062	Kinase insert domain protein receptor	24.00	106.7%	0.9997
42	D6	PPR43919A	*Klf4*	NM_053713	Kruppel-like factor 4 (gut)	23.21	104.9%	1.0000
43	D7	PPR50208A	*Lamb1*	XM_216679	Laminin, beta 1	24.56	113.2%	0.9995
44	D8	PPR63360A	*Lin28*	XM_575928	Lin-28 homolog (C. elegans)	22.98	104.5%	0.9997
45	D9	PPR44878A	*Ascl2*	NM_031503	Achaete-scute complex homolog 2 (Drosophila)	26.78	110.9%	0.9978
46	D10	PPR48578A	*Ascl1*	NM_022384	Achaete-scute complex homolog 1 (Drosophila)	24.84	126.0%	0.9994
47	D11	PPR65449A	*RGD1564419*	XM_575480	Similar to hypothetical gene supported by BC025338	25.04	131.7%	0.9999
48	D12	PPR63361A	*Myf5*	XM_235101	Myogenic factor 5	23.95	110.2%	0.9996
49	E1	PPR44362A	*Myod1*	NM_176079	Myogenic differentiation 1	24.98	112.1%	0.9990
50	E2	PPR59663A	*Nanog*	XM_575662	Nanog homeobox	24.05	113.9%	0.9995
51	E3	PPR44422A	*Nes*	NM_012987	Nestin	23.82	110.7%	0.9994

(*Continued*→)

TABLE 2. (CONTINUED)

No.	Position	Cat	Gene symbol	Refseq #	Official full name	Ct	E (%)	R
52	E4	PPR49735A	*Neurod1*	NM_019218	Neurogenic differentiation 1	26.39	91.2%	0.9999
53	E5	PPR43535A	*Nkx2-5*	NM_053651	NK2 transcription factor related, locus 5 (Drosophila)	25.63	110.9%	0.9990
54	E6	PPR57763A	*Nodal*	XM_228285	Nodal homolog (mouse)	23.73	129.3%	0.9990
55	E7	PPR52790A	*Nr2f1*	NM_031130	Nuclear receptor subfamily 2, group F, member 1	24.17	102.4%	1.0000
56	E8	PPR46535A	*Nr2f2*	NM_080778	Nuclear receptor subfamily 2, group F, member 2	23.96	108.0%	0.9997
57	E9	PPR59727A	*Pou5f1*	NM_001009178	POU class 5 homeobox 1	24.17	103.1%	0.9998
58	E10	PPR48805A	*Otx2*	XM_224009	Orthodenticle homolog 2 (Drosophila)	23.55	106.7%	0.9998
59	E11	PPR53060A	*Pax3*	XM_343601	Paired box 3	24.83	128.3%	0.9992
60	E12	PPR06696A	*Pdgfra*	XM_214030	Platelet-derived growth factor receptor, alpha polypeptide	24.25	111.0%	0.9992
61	F1	PPR50830A	*Pdx1*	NM_022852	Pancreatic and duodenal homeobox 1	24.02	108.3%	0.9998
62	F2	PPR57592A	*Pecam1*	NM_031591	Platelet/endothelial cell adhesion molecule 1	23.87	126.2%	0.9980
63	F3	PPR46507A	*Pitx2*	NM_019334	Paired-like homeodomain 2	23.53	118.6%	0.9995
64	F4	PPR06704A	*Ptn*	NM_017066	Pleiotrophin	24.74	106.6%	0.9999
65	F5	PPR61896A	*Zfp42*	XM_224882	Zinc finger protein 42	22.87	109.3%	0.9992
66	F6	PPR53039A	*Runx2*	XM_346016	Runt-related transcription factor 2	24.11	95.7%	0.9996
67	F7	PPR68948A	*LOC686412*	XM_001074001	Similar to sal-like 4 isoform a	25.30	97.3%	0.9998
68	F8	PPR44853A	*Shh*	NM_017221	Sonic hedgehog	26.71	110.5%	0.9998
69	F9	PPR47337A	*Epor*	NM_017002	Erythropoietin receptor	24.22	101.4%	0.9996
70	F10	PPR57227A	*Sox15*	XM_343921	SRY (sex determining region Y)-box 15	24.18	98.6%	0.9999
71	F11	PPR43961A	*Sox17*	XM_232640	SRY (sex determining region Y)-box 17	25.28	102.5%	0.9998
72	F12	PPR47353A	*Sox18*	NM_001024781	SRY (sex determining region Y)-box 18	25.54	116.6%	0.9990
73	G1	PPR60530A	*Sox2*	XM_574919	SRY (sex determining region Y)-box 2	25.34	106.8%	0.9996
74	G2	PPR55616A	*Sox7*	XM_224283	SRY (sex determining region Y)-box 7	24.13	108.3%	0.9991
75	G3	PPR53743A	*Sparc*	NM_012656	Secreted protein, acidic, cysteine-rich (osteonectin)	24.39	100.0%	1.0000
76	G4	PPR44745A	*Stat3*	NM_012747	Signal transducer and activator of transcription 3	24.22	126.5%	0.9980
77	G5	PPR68944A	*RGD1559950*	XM_573971	RGD1559950 similar to STELLA	22.50	101.9%	0.9999
78	G6	PPR49061A	*Tbx2*	XM_220810	T-box 2	26.70	93.6%	0.9997
79	G7	PPR53340A	*Tbx3*	NM_181638	T-box 3	24.09	112.7%	0.9995
80	G8	PPR59824A	*Tbx5*	NM_001009964	T-box 5	25.84	103.3%	0.9993
81	G9	PPR66677A	*Tcl1a*	XM_001068183	T-cell leukemia/lymphoma 1A	24.20	104.9%	1.0000
82	G10	PPR50309A	*Tert*	NM_053423	Telomerase reverse transcriptase	24.25	108.4%	0.9995
83	G11	PPR49669A	*Tubb3*	NM_139254	Tubulin, beta 3	23.83	102.9%	0.9999
84	G12	PPR68393A	*Utf1*	XM_001058894	Undifferentiated embryonic cell transcription factor 1	23.61	101.3%	1.0000
85	H1	PPR42363A	*Rplp1*	NM_001007604	Ribosomal protein, large, P1	23.33	101.9%	1.0000
86	H2	PPR42247A	*Hprt1*	NM_012583	Hypoxanthine phosphoribosyltransferase 1	25.02	108.5%	0.9986
87	H3	PPR53027A	*Rpl13a*	NM_173340	Ribosomal protein L13A	21.42	107.7%	0.9990
88	H4	PPR56603A	*Ldha*	NM_017025	Lactate dehydrogenase A	21.90	119.2%	0.9996
89	H5	PPR06557A	*Gapdh*	NM_017008	Glyceraldehyde-3-phosphate dehydrogenase	16.55	123.3%	0.9995
90	H6	PPR63338A	*RGDC*	U26919	Rat Genomic DNA Contamination	23.73	101.9%	1.0000
91	H7	PPX63340A	*RTC*	SA_00104	Reverse transcription control	21.95	107.2%	1.0000
92	H8	PPX63340A	*RTC*	SA_00104	Reverse transcription control	21.50	102.5%	1.0000
93	H9	PPX63340A	*RTC*	SA_00104	Reverse transcription control	21.44	105.4%	0.9992
94	H10	PPX63339A	*PPC*	SA_00103	Positive PCR control	18.80	110.9%	0.9997
95	H11	PPX63339A	*PPC*	SA_00103	Positive PCR control	18.74	108.6%	0.9997
96	H12	PPX63339A	*PPC*	SA_00103	Positive PCR control	18.70	103.6%	0.9998

Qiagen catalog number: CAPR10083, Plate format: 96×1, Real-time instrument: iQ5.

The genes *Ctnnbl1*, *Pias1*, *Hdac2*, *Myod1*, *Neurod1*, and *Sox18* were found to be good candidates for replacement since they did not discriminate cell types. In contrast, the genes *Nanog*, *Afp*, *Gdf3*, *Stella*, *Oct4*, *Utf1*, *Fgf4*, and *Cer1* were able to differentiate cell lines and conditions (see Supplementary Table S1 and Fig. 4).

Discussion

The ability to rapidly analyze gene expression in rat ESC lines using a focused gene array will facilitate the optimization of medium conditions, the characterization of new ESC lines, and confirm that the ESC lines maintain their

undifferentiated state. Here, we describe such an array and evaluated its utility to discriminate undifferentiated rat ESC lines from differentiated ESCs (e.g., ESCs differentiated to EB for 5 or 10 days), from other cells derived from rat embryos such as TS cells and XEN cells, and from MEFs. This array had good inter-operator reproducibility (shown in Fig. 1) and has good QC/QA tools. This focused array produced rapid and reproducible results in a convenient, inexpensive format. Thus, this array will have broad application for laboratories wishing to characterize or optimize rat ESC culture.

When overall gene expression was analyzed, the gene array could discriminate undifferentiated genuine rat ESCs grown from TS, XEN, or MEFs. When overall gene expression was analyzed, the array discriminated undifferentiated rat ESCs grown in 2i plus LIF from rat ESCs that were differentiated for 10 days to EBs. When the expression of individual genes that are highly expressed by undifferentiated ESCs or genes highly expressed during the first 5 to 10 days of differentiation are explored, the array resolved undifferentiated ESCs from EBs differentiated for 5 or 10 days.

The biology of rat ESCs

Currently, the biological differences between mouse, human, and rat ESCs are not well understood. For example, as shown in Fig. 4, undifferentiated, genuine rat ESCs derived in 2i plus LIF and those derived in 4i medium express *Cdx2* and other genes of the trophoblast lineage such as *Hand1* and *Eomes* [7,8,19]. Previously, Cdx2 protein expression in rat ESCs was demonstrated by immunocytochemistry, so it is unlikely this is a false positive [6]. We also noted that Cdx2 expression appears to be >3-fold higher in genuine rat ESCs maintained in 4i (YPAC) conditions compared with 2i plus LIF conditions (see Fig. 4). In fact, genuine rat ESCs derived and maintained in 4i medium had higher expression of *Cdx2* than TS cells. In contrast to *Cdx2* where the expression levels did not discriminate ESCs and TS cells well, TS cells express *Hand1*, *Fgf4*, and *Eomes* at higher levels than genuine rat ESCs. Despite Cdx2 expression by genuine rat ESCs, the array differentiated XEN and TS cells from ESCs based on the expression of *Nanog*, *Pou5f1*, *Fgf4*, *Sox2*, and others (see Fig. 3C). For example, the expression of *Nanog* was >10,000-fold higher in ESCs than either XEN or TS cells. In summary, the expression of *Nanog*, *Oct4*, and *Fgf4* by ESCs and not by XEN and TS cells together with expression of *Gata4* and *Gata6* by XEN and *Hand1* by TS, distinguish XEN and TS cells from ESCs [7,16,18,26].

Since rat ESCs grown in 2i+LIF or 4i are not as efficient at germline transmission as seen in certain mouse strains, we hypothesize that culture conditions that activate or maintain Cdx2 expression might cause rat ESCs to contribute to extraembryonic tissues. This suggests that rat ESCs may contribute to extraembryonic tissues in addition to the inner cell mass following blastocyst injection. Therefore, culture conditions that decrease *Cdx2* gene expression might increase ESC contribution to the inner cell mass and subsequently increase germline transmission efficiency. Further work is needed to confirm this hypothesis.

Technical considerations

The array has elements for QA and QC including 3 elements each for PPC and RTE controls, and an RGDC element. Using the manufacturer's criteria, in 2 arrays, RGDC was questionable. In each case, the technical replicate did not detect RGDC. To further resolve this finding, RT-PCR was performed using a set of primers for Pbgd (also known as Hmbs) that span an intron. The results were unable to verify RGDC. We speculate that the manufacturer's criteria for evaluation of RGDC may generate false positives at a frequency of ~8%. Regarding QA/QC, we noted a tendency for the RNeasy method of total RNA isolation to produce more uniform results compared to the TRIZOL method (see Fig. 1B). A similar observation was noted in the Troubleshooting section of the user's manual provided by the manufacturer. Therefore, it is recommended that a qPCR Grade RNA Isolation Kit be employed with DNase treatment to maximize reproducibility of array findings.

Limitations of this array

Here, we used an array with 86 unique elements. Therefore, there are limitations in terms of the breadth of gene expression information obtained compared with a more global gene expression such as that previously obtained using the Affymetrix rat expression system whose probe set contains >30,000 elements [26]. In their analysis, Li et al. derived and maintained rat ESC-like cells in a medium containing LIF and GSK inhibitor (note their ESC-like cells were shown to form teratoma and to be alkaline phosphatase-positive; they did not test whether their ESC-like cells were competent to contribute to chimera or germline transmission). It is worth pointing out that some of the known pluripotency genes, such as *Tbx3* and *Stella* (Dppa3) were shown to be expressed at high levels in their analysis [26], as was shown to be expressed here (see Table 2). Also, we noted that the primitive endoderm cells that were derived from their rat ESC-like cells expressed high levels of *Gata6*, *Gata4*, *Sox17*, and *Foxa2* [26], similar to what we demonstrated here for the XEN cells (see Fig. 3C, Supplementary Table S4).

In an overall analysis using all genes on the array, the array did not discriminate undifferentiated rat ESCs from EBs differentiated for 5 days. However, genes that are strongly induced by differentiation, such as *Cer1*, *Afp*, *Actc1*, *Foxa2*, *Gata4*, *Gata6*, *Hand1*, *Sox7*, *Sox17*, and *Pdx1*, or particular genes that are strongly downregulated by differentiation, such as *Gdf3* and*Tcl1a*, distinguish rat ESCs that were differentiated for 5 days to EBs from undifferentiated rat ESCs (see Fig. 3B).

Previous work has indicated that expression of certain genes such as *Nanog*, *Oct4*, or *Stella* [17,27–30], epigenetic or microRNA differences [11,31–35] might enrich germline ESCs from other ESCs. Here, the array did not discriminate undifferentiated rat ESC lines that form chimera from genuine rat ESC lines. In fact, no genes were found to be expressed >10-fold difference between chimera 2i ESCs and germline 2i ESCs (see Fig. 3D). Therefore, the role of Dlk1-Dio3 region [34] or the role of miRNAs such as miR-290 miRNA cluster [36–39] might be targets to investigate in rat ESCs in future work.

Acknowledgments

The authors thank Kristin Whiteside, Joseph Smith, and Drs. Brian Petroff, Jay Vivian, and David Albertini for their

encouragement and assistance with this work. Dr. Dan Marcus and COBRE grant NIH/NCRR P20-RR017686 are thanked for use of the Nanodrop. This work was supported by grants from the Johnson Center for Cancer Research, the National Institutes of Health [NS34160 (M.L.W.) and HD020676 (M.J.S.)], the Kansas Biosciences Authority, the University of Kansas Cancer Center pilot project program 2010, the KSU College of Veterinary Medicine Dean's office, and by the State of Kansas Legislature to the Midwest Institute for Comparative Stem Cell Biology. A portion of this work was supported by the Deffenbaugh Foundation to the Spinal Cord Injury Program at the University of Kansas Medical School. MLW thanks BGW for her lifelong support. Mr. and Mrs. Howard Walker are thanked for their hospitality during the fall of 2010.

Author Disclosure Statement

The authors indicate no potential conflicts of interest.

References

1. Hamra FK. (2010). Gene targeting: enter the rat. Nature 467:161–163.
2. Iannaccone PM and HJ Jacob. (2009). Rats! Dis Model Mech 2:206–210.
3. Buehr M, S Meek, K Blair, J Yang, J Ure, J Silva, R McLay, J Hall, QL Ying and A Smith. (2008). Capture of authentic embryonic stem cells from rat blastocysts. Cell 135: 1287–1298.
4. Li P, C Tong, R Mehrian-Shai, L Jia, N Wu, Y Yan, RE Maxson, EN Schulze, H Song, et al. (2008). Germline competent embryonic stem cells derived from rat blastocysts. Cell 135:1299–1310.
5. Tong C, P Li, NL Wu, Y Yan and QL Ying. (2010). Production of p53 gene knockout rats by homologous recombination in embryonic stem cells. Nature 467:211–213.
6. Hong J, H He and ML Weiss. (2011). Derivation and characterization of embryonic stem cells lines derived from transgenic fischer 344 and dark agouti rats. Stem Cells Dev 21:1571–1586.
7. Ralston A and J Rossant. (2005). Genetic regulation of stem cell origins in the mouse embryo. Clin Genet 68:106–112.
8. Sasaki H. (2010). Mechanisms of trophectoderm fate specification in preimplantation mouse development. Dev Growth Differ 52:263–273.
9. Buehr M, J Nichols, F Stenhouse, P Mountford, CJ Greenhalgh, S Kantachuvesiri, G Brooker, J Mullins and AG Smith. (2003). Rapid loss of Oct-4 and pluripotency in cultured rodent blastocysts and derivative cell lines. Biol Reprod 68:222–229.
10. Kawamata M and T Ochiya. (2010). Generation of genetically modified rats from embryonic stem cells. Proc Natl Acad Sci U S A 107:14223–14228.
11. Aiba K, T Nedorezov, Y Piao, A Nishiyama, R Matoba, LV Sharova, AA Sharov, S Yamanaka, H Niwa and MS Ko. (2009). Defining developmental potency and cell lineage trajectories by expression profiling of differentiating mouse embryonic stem cells. DNA Res 16:73–80.
12. Tanaka TS, T Kunath, WL Kimber, SA Jaradat, CA Stagg, M Usuda, T Yokota, H Niwa, J Rossant and MS Ko. (2002). Gene expression profiling of embryo-derived stem cells reveals candidate genes associated with pluripotency and lineage specificity. Genome Res 12:1921–1928.
13. Chuykin I, I Lapidus, E Popova, L Vilianovich, V Mosienko, N Alenina, B Binas, G Chai, M Bader and A Krivokharchenko. (2010). Characterization of trophoblast and extraembryonic endoderm cell lineages derived from rat preimplantation embryos. PLoS One 5:e9794.
14. Debeb BG, V Galat, J Epple-Farmer, S Iannaccone, WA Woodward, M Bader, P Iannaccone and B Binas. (2009). Isolation of Oct4-expressing extraembryonic endoderm precursor cell lines. PLoS One 4:e7216.
15. Galat V, B Binas, S Iannaccone, LM Postovit, BG Debeb and P Iannaccone. (2009). Developmental potential of rat extraembryonic stem cells. Stem Cells Dev 18:1309–1318.
16. Brons IG, LE Smithers, MW Trotter, P Rugg-Gunn, B Sun, SM Chuva de Sousa Lopes , SK Howlett, A Clarkson, L Ahrlund-Richter, RA Pedersen and L Vallier. (2007). Derivation of pluripotent epiblast stem cells from mammalian embryos. Nature 448:191–195.
17. Hayashi K, SM Lopes, F Tang and MA Surani. (2008). Dynamic equilibrium and heterogeneity of mouse pluripotent stem cells with distinct functional and epigenetic states. Cell Stem Cell 3:391–401.
18. Tesar PJ, JG Chenoweth, FA Brook, TJ Davies, EP Evans, DL Mack, RL Gardner and RD McKay. (2007). New cell lines from mouse epiblast share defining features with human embryonic stem cells. Nature 448:196–199.
19. Asanoma K, MA Rumi, LN Kent, D Chakraborty, SJ Renaud, N Wake, DS Lee, K Kubota and MJ Soares. (2011). FGF4-dependent stem cells derived from rat blastocysts differentiate along the trophoblast lineage. Dev Biol 351:110–119.
20. Tanaka S, T Kunath, AK Hadjantonakis, A Nagy and J Rossant. (1998). Promotion of trophoblast stem cell proliferation by FGF4. Science 282:2072–2075.
21. Soares MJ, KD Schaberg, CS Pinal, SK De, P Bhatia and GK Andrews. (1987). Establishment of a rat placental cell line expressing characteristics of extraembryonic membranes. Dev Biol 124:134–144.
22. Vandesompele J, PK De, F Pattyn, B Poppe, RN Van, PA De and F Speleman. (2002). Accurate normalization of real-time quantitative RT-PCR data by geometric averaging of multiple internal control genes. Genome Biol 3:RESEARCH0034.
23. Andersen CL, JL Jensen and TF Orntoft. (2004). Normalization of real-time quantitative reverse transcription-PCR data: a model-based variance estimation approach to identify genes suited for normalization, applied to bladder and colon cancer data sets. Cancer Res 64:5245–5250.
24. Pfaffl MW, A Tichopad, C Prgomet and TP Neuvians. (2004). Determination of stable housekeeping genes, differentially regulated target genes and sample integrity: BestKeeper—Excel-based tool using pair-wise correlations. Biotechnol Lett 26:509–515.
25. Silver N, S Best, J Jiang and SL Thein. (2006). Selection of housekeeping genes for gene expression studies in human reticulocytes using real-time PCR. BMC Mol Biol 7:33.
26. Li C, Y Yang, J Gu, Y Ma and Y Jin. (2009). Derivation and transcriptional profiling analysis of pluripotent stem cell lines from rat blastocysts. Cell Res 19:173–186.
27. Chambers I, J Silva, D Colby, J Nichols, B Nijmeijer, M Robertson, J Vrana, K Jones, L Grotewold and A Smith. (2007). Nanog safeguards pluripotency and mediates germline development. Nature 450:1230–1234.
28. Tanaka TS, DS Lopez, I Lopez de Silanes, LV Sharova, H Akutsu, T Yoshikawa, H Amano, S Yamanaka, M Gorospe and MS Ko. (2006). Esg1, expressed exclusively in preimplantation embryos, germline, and embryonic stem cells, is a

putative RNA-binding protein with broad RNA targets. Dev Growth Differ 48:381–390.
29. Yeom YI, G Fuhrmann, CE Ovitt, A Brehm, K Ohbo, M Gross, K Hubner and HR Scholer. (1996). Germline regulatory element of Oct-4 specific for the totipotent cycle of embryonal cells. Development 122:881–894.
30. Scholer HR, AK Hatzopoulos, R Balling, N Suzuki and P Gruss. (1989). A family of octamer-specific proteins present during mouse embryogenesis: evidence for germline-specific expression of an Oct factor. EMBO J 8:2543–2550.
31. Bao S, F Tang, X Li, K Hayashi, A Gillich, K Lao and MA Surani. (2009). Epigenetic reversion of post-implantation epiblast to pluripotent embryonic stem cells. Nature 461: 1292–1295.
32. Imamura M, K Miura, K Iwabuchi, T Ichisaka, M Nakagawa, J Lee, M Kanatsu-Shinohara, T Shinohara and S Yamanaka. (2006). Transcriptional repression and DNA hypermethylation of a small set of ES cell marker genes in male germline stem cells. BMC Dev Biol 6:34.
33. Surani MA, G Durcova-Hills, P Hajkova, K Hayashi and WW Tee. (2008). Germ line, stem cells, and epigenetic reprogramming. Cold Spring Harb Symp Quant Biol 73:9–15.
34. Liu L, GZ Luo, W Yang, X Zhao, Q Zheng, Z Lv, W Li, HJ Wu, L Wang, XJ Wang and Q Zhou. (2010). Activation of the imprinted Dlk1-Dio3 region correlates with pluripotency levels of mouse stem cells. J Biol Chem 285:19483–19490.
35. Melton C, RL Judson and R Blelloch. (2010). Opposing microRNA families regulate self-renewal in mouse embryonic stem cells. Nature 463:621–626.
36. Babiarz JE, JG Ruby, Y Wang, DP Bartel and R Blelloch. (2008). Mouse ES cells express endogenous shRNAs, siRNAs, and other Microprocessor-independent, Dicer-dependent small RNAs. Genes Dev 22:2773–2785.
37. Judson RL, JE Babiarz, M Venere and R Blelloch. (2009). Embryonic stem cell-specific microRNAs promote induced pluripotency. Nat Biotechnol 27:459–461.
38. Luningschror P, B Stocker, B Kaltschmidt and C Kaltschmidt. (2012). miR-290 cluster modulates pluripotency by repressing canonical NF-kappaB signaling. Stem Cells 30: 655–664.
39. Pfaff N, T Moritz, T Thum and T Cantz. (2012). miRNAs involved in the generation, maintenance, and differentiation of pluripotent cells. J Mol Med (Berlin) 90:747–752.

Address correspondence to:
Dr. Mark L. Weiss
Department of Anatomy and Physiology
Kansas State University College of Veterinary Medicine
Coles Hall
Room 105
Manhattan, KS 66506

E-mail: mlweiss@ksu.edu

Received for publication May 23, 2012
Accepted after revision August 7, 2012
Prepublished on Liebert Instant Online August 14, 2012

SCIENTIFIC REPORTS

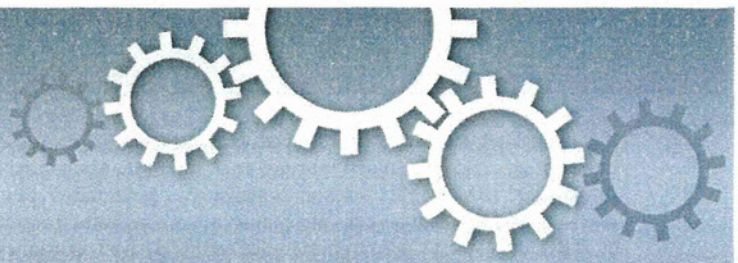

OPEN

SUBJECT AREAS:
PROTEIN DELIVERY
MESENCHYMAL STEM CELLS
MOLECULAR NEUROSCIENCE
PROTEASES

Received
17 October 2012

Accepted
15 January 2013

Published
1 February 2013

Correspondence and requests for materials should be addressed to T.O. (tochiya@ncc.go.jp)

Human adipose tissue-derived mesenchymal stem cells secrete functional neprilysin-bound exosomes

Takeshi Katsuda[1,2], Reiko Tsuchiya[3], Nobuyoshi Kosaka[1], Yusuke Yoshioka[1], Kentaro Takagaki[3], Katsuyuki Oki[3], Fumitaka Takeshita[1], Yasuyuki Sakai[2], Masahiko Kuroda[4] & Takahiro Ochiya[1]

[1]From the Division of Molecular and Cellular Medicine, National Cancer Center Research Institute, 5-1-1 Tsukiji, Chuo-ku, Tokyo 104-0045, Japan, [2]Institute of Industrial Science (IIS), The University of Tokyo, 4-6-1 Komaba, Meguro-ku, Tokyo 153-8505, Japan, [3]Research and Development Dept., SEEMS Inc., 2-4-32 Aomi, Koto-ku, Tokyo 135-0064, Japan, [4]Department of Pathology, Tokyo Medical University, 6-1-1, Shinjuku, Shinjuku-ku, Tokyo, 160-8402, Japan.

Alzheimer's disease (AD) is characterized by the accumulation of β-amyloid peptide (Aβ) in the brain because of an imbalance between Aβ production and clearance. Neprilysin (NEP) is the most important Aβ-degrading enzyme in the brain. Thus, researchers have explored virus-mediated NEP gene delivery. However, such strategies may entail unexpected risks, and thus exploration of a new possibility for NEP delivery is also required. Here, we show that human adipose tissue-derived mesenchymal stem cells (ADSCs) secrete exosomes carrying enzymatically active NEP. The NEP-specific activity level of 1 μg protein from ADSC-derived exosomes was equivalent to that of ~ 0.3 ng of recombinant human NEP. Of note, ADSC-derived exosomes were transferred into N2a cells, and were suggested to decrease both secreted and intracellular Aβ levels in the N2a cells. Importantly, these characteristics were more pronounced in ADSCs than bone marrow-derived mesenchymal stem cells, suggesting the therapeutic relevance of ADSC-derived exosomes for AD.

Alzheimer's disease (AD) is a progressive and fatal neurodegenerative disorder that is characterized by memory loss and cognitive ability deterioration. The accumulation of β-amyloid peptide (Aβ) in the brain plays a critical role in AD pathogenesis[1,2]. The steady-state level of Aβ is determined by a balance between its biosynthesis and clearance[3]. The physiological metabolite Aβ is constantly produced and removed in the brain, and it has been demonstrated that even small decreases in its removal lead to Aβ deposition[3]. Among several proteases involved in the proteolysis of Aβ, neprilysin (neutral endopeptidase: NEP), a type II membrane-associated metalloendopeptidase, appears to be the most important[4,5]. Indeed, AD patients show decreased expression and activity of NEP[6]. Thus, NEP has been intensively studied as a potential therapeutic target for AD[7]. One promising approach for lowering brain Aβ levels is the delivery of NEP. Recent reports have indicated that NEP gene delivery either peripherally or within the brain is effective in clearing brain Aβ[7]. However, safety issues related to the use of viral vectors limit the feasibility of this approach.

NEP, more often referred to as CD10, is expressed by mesenchymal stem cells (MSCs)[8,9]. However, to our knowledge, no study has explored the therapeutic potential of MSCs with regard to their Aβ degrading capacity. MSCs initially attracted interest for their ability to differentiate into cells of mesodermal lineage *in vitro* and *in vivo*[11]. Furthermore, in the last decade, it has been demonstrated that MSCs have many other functional properties. They can differentiate into cells from unrelated germline lineages, resist immunosurveillance, home to injured tissue, and secrete factors with immunosuppressive, anti-apoptotic, and trophic effects[10,11]. Accordingly, there is growing evidence that MSC-based therapies could benefit a wide range of neurodegenerative diseases[12], including AD[13–18]. The mechanisms by which transplanted MSCs influence AD have been roughly classified as cellular replacement[13,14] or paracrine secretion[15–18], but the precise mechanism remains unclear. Thus, any possible mechanism of AD pathophysiology should be investigated, and any possible strategy for AD treatment should be explored.

Another recently reported remarkable feature of MSCs is their ability to secrete exosomes with therapeutic potential[19]. Exosomes are small, intraluminal vesicles of multivesicular bodies released when they fuse with the plasma membrane[20]. It has been suggested that these vesicles are produced by a variety of cell types and can function as intercellular transmitters of mRNA, microRNA, and proteins[21–23]. The first evidence of the

therapeutic potential of MSC-derived exosomes was in a mouse model of acute kidney injury[24]. Bruno et al. found that bone marrow-derived (BM−) MSC exosomes activated a proliferative program in surviving tubular cells after injury via a horizontal transfer of mRNA. Lai et al. also reported that MSC-derived exosomes exerted therapeutic effects on myocardial ischemia/reperfusion injury[25].

Given that exosomes are membrane vesicles and that MSCs express membrane-bound enzyme NEP, it can be assumed that MSCs would secrete exosomes with NEP on their membrane. Here, we report for the first time that adipose tissue-derived MSCs (ADSCs) produce NEP-bound exosomes approximately 100–200 nm in diameter. Furthermore, co-culture of N2a cells overproducing human Aβ with ADSCs led to decreases in the secreted Aβ40 and 42 levels as well as a decrease in the intracellular Aβ42 level. Importantly, these characteristics were more pronounced in ADSCs than BM-MSCs, suggesting the therapeutic relevance of ADSC-derived exosomes for AD.

Results

ADSCs express NEP at a higher level than BM-MSCs. To select the optimal source of MSCs for the present study, we performed comparative analyses on NEP expression between ADSCs and BM-MSCs. A flow cytometry analysis indicated that NEP-positive populations in ADSCs were greater than those in BM-MSCs (Fig. 1A); regarding the other surface markers, they showed the similar profiles that are characteristic to MSCs (positive for CD105, CD73, CD90, and CD44; negative for CD45, CD31, and CD34) (Fig. S1). By qRT-PCR analysis, we confirmed that NEP gene expression levels were considerably higher in ADSCs from each donor than in BM-MSCs from all 4 donors (Fig. 1B). In addition, immunoblot analysis revealed that the NEP protein expression level in ADSCs was ~ 4-fold higher than that of BM-MSCs (Fig. 1C). This observation was further confirmed by immunocytochemistry, where ADSCs were stained for NEP more strongly than BM-MSCs (Fig. 1D). Collectively, these results demonstrate that ADSCs express more NEP than BM-MSCs. Thus, we mainly focused on ADSCs for the subsequent experiments.

ADSC-derived NEP exhibits specific enzyme activity. To investigate the feasibility of using ADSC-derived NEP as a therapeutic target, we examined whether ADSCs indeed exhibited NEP-specific enzyme activity. We measured NEP-specific enzyme activity using a fluorogenic peptide substrate, Mca-RPPGFSAFK(Dnp), and a selective NEP inhibitor, thiorphan. This substrate can be cleaved by several endopeptidases, including NEP, endothelin-converting enzyme (ECE)-1, ECE-2, angiotensin-converting enzyme (ACE)-1, ACE-2, and insulin-degrading enzyme (IDE)[26]. However, at pH 7.5, the use of thiorphan allows the discrimination of NEP enzyme activity from other closely related enzymes[26].

Cell lysates of ADSCs from each donor exhibited enzyme activity both in the presence and absence of thiorphan (Figs. S2 A-D). NEP-specific activity, calculated after the subtraction of fluorescence in the presence of thiorphan, demonstrated that all ADSCs exhibited NEP-specific enzyme activity (Fig. 2A). NEP-specific enzyme activity accounted for 38.3 ± 4.5% of total enzyme activity (Fig. 2B), and the activity level of 1 μg ADSC cell lysate was estimated to be equivalent to that of 0.35 ± 0.14 ng recombinant human NEP (rhNEP) (Fig. 2C, termed as NEP activity index). In contrast to the above observation, BM-MSCs showed weak or undetectable NEP enzyme activity (Fig. 2D). Intriguingly, the total enzyme activity of BM-MSCs measured in the absence of thiorphan was comparable to that of ADSCs (Figs. S3 A, B). That is, NEP-specific enzyme activity contributed relatively little to the total enzyme activity of BM-MSCs (Fig. 2D), suggesting that NEP activity is a unique characteristic of ADSCs. These results support the idea that NEP expressed by ADSCs, but not BM-MSCs, may be therapeutically useful for AD.

ADSCs secrete exosomes to their culture supernatant. Recently, it has been shown that exosomes secreted by MSCs contribute to their paracrine effects[19,25,26]. Considering the reports that transplanted MSCs influenced AD via their paracrine effects[15–18], we hypothesized that ADSC-derived exosomes would have therapeutic potential for AD, especially by focusing on their NEP producing ability.

To test whether ADSCs could secrete NEP via exosome release, we isolated putative exosome fractions from conditioned media of ADSCs from 4 donors (#1–4) with a standard ultracentrifugation method[27,28]. The phase-contrast electron micrographs of the exosomes revealed rounded and double-membraned structures with a size of approximately 60–200 nm (Fig. 3A). Immunoblot analyses revealed that tetraspanin CD81, a reliable exosomal marker[29], was present in the exosome fraction but absent in the donor cell lysates (Fig. 3B). We also confirmed the presence of CD63, another well-established exosome marker[29] (Fig. 3B). CD63 was also detected in the cell lysate, but this is in accordance with the fact that CD63 is expressed by MSCs[30]. In contrast, cellular proteins cytochrome c and actin were detected exclusively in the cell lysates (Fig. 3B). Then, we analyzed the size distribution of the isolated exosomes by two distinct methods: NTA and scanning ion occlusion sensing (SIOS). The size distribution was physically homogeneous with a peak at 150–200 nm, as determined by nanoparticle tracking analysis (NTA) (Fig. 3C, E), or at 110–160 nm, as determined by SIOS (Fig. 3D, E). The size of ADSC-derived exosomes was relatively larger than that of previously reported exosomes, which were 50–100 nm in diameter. The exosome yield per 10^6 ADSCs per day was 1–4 × 10^8 particles, as determined by NTA, or 1–4 μg protein, as determined by the Bradford method (Fig. 3E). Collectively, these results reveal that ADSCs secrete exosomes to the culture supernatant.

ADSC-derived exosomes contain enzymatically active NEP. It is thought that the molecular composition of exosomes reflects the specialized functions of their original cells[19,31]. Thus, we next asked whether ADSC-derived exosomes contained enzymatically active NEP. Immunoblot analyses revealed that exosomes secreted by each line of donor-derived ADSCs contained NEP (Fig. 4A). Of note, the enzyme activity assay using a fluorogenic substrate revealed that these exosomes exhibited NEP-specific activity (Fig. 4B). Interestingly, comparison of exosomal enzyme activity in the presence and absence of thiorphan demonstrated that NEP-specific activity accounted for a large proportion of the total activity (Fig. 4C, D): the enzyme activity was almost completely lost in the presence of thiorphan (Fig. 4D). The NEP-specific activity / total activity ratios of ADSC-derived exosomes reached 89.5 ± 4.4% (Fig. 4E). NEP-specific activity level of 1 μg protein from ADSC-derived exosomes was estimated to be equivalent to 0.26 ± 0.07 ng rhNEP (Fig. 4F, Fig. 4S). In addition, we confirmed that ADSC-derived exosomes exhibited a higher NEP-specific activity than BM-MSC-derived esosomes (Fig. 4G). These results demonstrate that ADSC-derived exosomes possess enzymatically active NEP, implying that they can serve as a novel NEP protein delivery system.

ADSCs decrease both the extracellular and intracellular Aβ levels of N2a cells. To test whether ADSCs could contribute to decrease of both synthesized and secreted Aβ, we co-cultured ADSCs or BM-MSCs with a neuroblastoma cell line N2a cells genetically modified to overproduce human Aβ (Fig. 5A)[32]. Both Aβ40 and 42 levels in the N2a cell culture media were significantly decreased after co-culture with ADSCs or BM-MSCs (Fig. 5B, C). The decreasing degrees of both secreted Aβ40 and 42 levels were greater in co-culture with ADSCs than BM-MSCs (Fig. 5B, C). Of note, we also found that

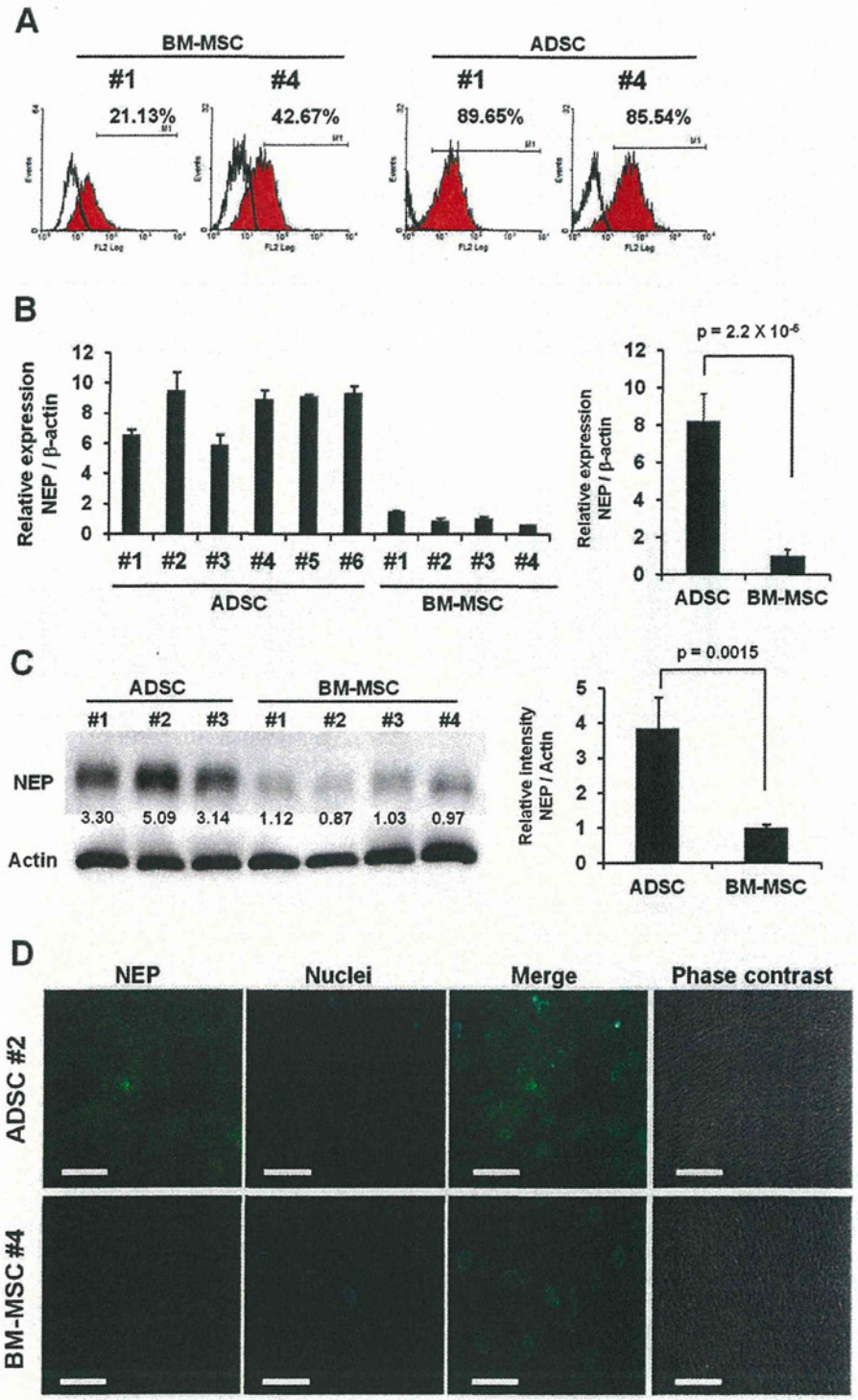

Figure 1 | ADSCs express NEP at a higher level than BM-MSCs. (A) Flow cytometry results of ADSCs #1 and #4 and BM-MSCs #1 and #4 for NEP. (B) qRT-PCR analysis of NEP in ADSCs and BM-MSCs. Transcript levels were normalized to β-actin levels. Data are the mean ± S.D. (n = 3). (C) Cell lysates of ADSCs or BM-MSCs were analyzed by immunoblotting with an anti-NEP or an anti-actin antibody (left). Either 3 μg or 1 μg of cell lysate protein per lane was loaded for NEP and actin, respectively. The relative signal intensity (NEP/Actin) for each sample was measured, and normalized values are shown in the graph. The average values of ADSCs and BM-MSCs are compared on the right. Data are the mean ± S.D. (D) Immuno cytochemistry of ADSCs for NEP. ADSCs were stained with a mouse-anti NEP monoclonal antibody (green), and nuclei were counterstained with Hoechst 33342 (blue). Scale bar: 50 μm.

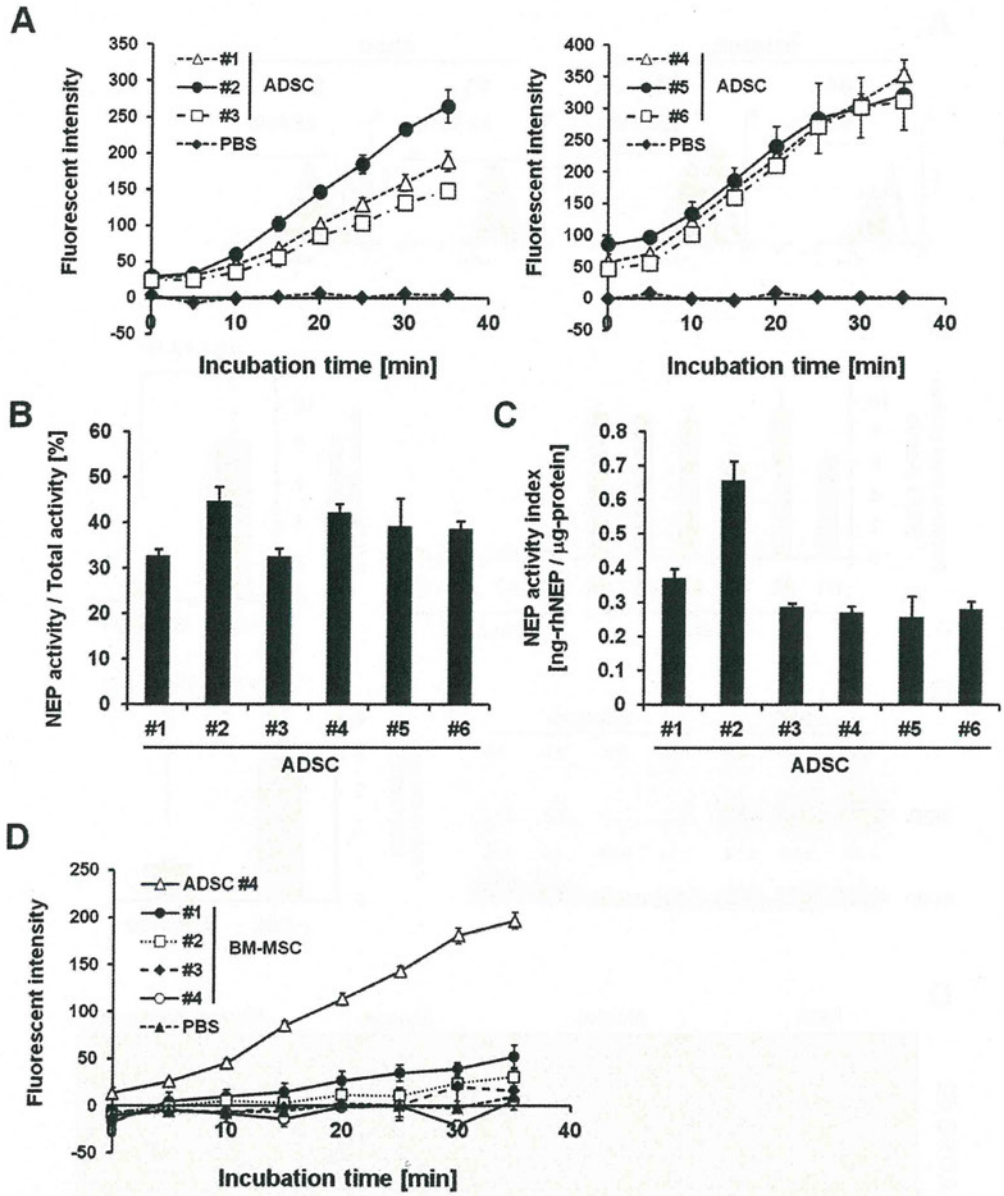

Figure 2 | ADSCs, but not BM-MSCs, exhibit NEP-specific enzyme activity. (A) NEP-specific enzyme activity was measured in ADSC cell lysates (left: #1–3 and right: #4–6) using a fluorogenic peptide substrate, Mca-RPPGFSAFK(Dnp). The average NEP activity represented by fluorescence intensity was measured with a reading interval of 5 min. The specific NEP activity was calculated by subtracting residual fluorescent intensity after incubation with the NEP inhibitor thiorphan (Fig. S2 A–D). Data are the mean ± S.D. (n = 3). (B) NEP contribution ratio calculated as the percentage ratio of NEP-specific activity rate to total activity rate. NEP-specific or total enzyme activity rate was determined as the gradient of the corresponding time course of fluorescent intensity. Data are the mean ± S.D. (n = 3). (C) NEP-specific enzyme activity levels of ADSCs were estimated from rhNEP standard curves (Fig. S2 E–H) and represented as the value ng-rhNEP/µg-protein (termed as NEP activity index in the diagram). Data are the mean ± S.D. (n = 3). (D) Comparison of NEP-specific enzyme activity levels between ADSC #4 and BM-MSCs #1–4. Data are the mean ± S.D. (n = 3).

the intracellular Aβ42 level in N2a cells was significantly decreased by co-culture with ADSCs or BM-MSCs (Fig. 5D). This suggests that NEP-loaded exosomes secreted by ADSCs or BM-MSCs entered the cytoplasm of N2a cells, and degraded the intracellular Aβ of N2a cells. Indeed, addition of thiorphan raised the intracellular Aβ42 level from 77% to 92% of that of the control (Fig. 5E). We also confirmed that ADSC-derived exosomes, at least in part, contributed to decreasing the intracellular Aβ42 level in N2a cells (Fig. S5).

ADSC-derived exosomes are incorporated into neuroblastoma cells. To verify that ADSC transferred their exosomes to N2a cells, we co-cultured PKH26 labeled ADSCs with PKH67 labled N2a cells (Fig. 6A). One day after co-culture, some, but not all, N2a cells were co-stained with PKH26 and PKH67, suggesting that exosomes secreted by ADSCs were transferred to N2a cells (Fig. 6A). Interestingly, however, we did not observe co-stained ADSCs, suggesting a certain mechanism underlying the unidirectional transport of exosomes from ADSCs to N2a cells, but not from N2a cells to ADSCs. Exosomal membrane is rich in ceramide, which may lead to inefficient incorporation of the cell membrane-linked PKH into the secreted exosomes[33]. Thus, we next directly labeled ADSC-derived exosomes with PKH67, and examined whether these

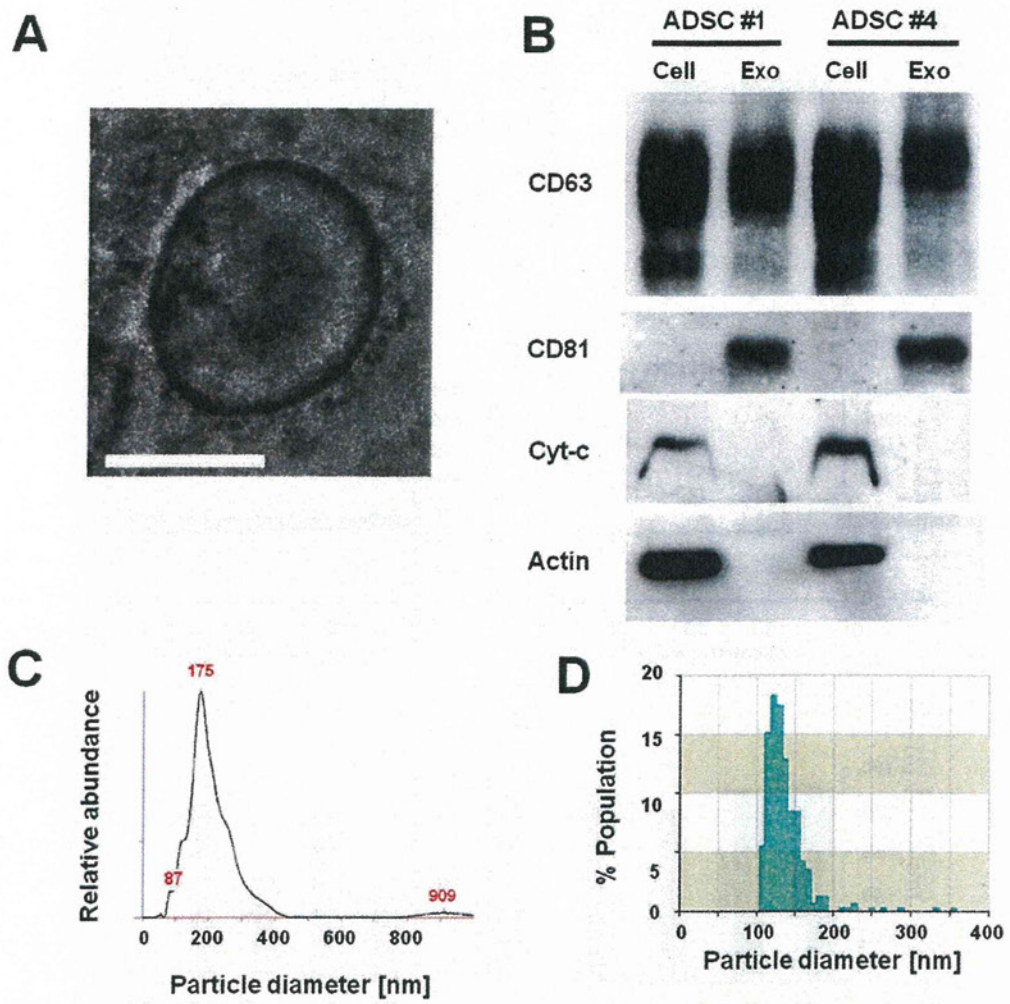

E

		Yield [/ 10^6 cells / d]		Peak diameter [nm]	
		Protein [μg]	X 10^8 Particles	By NTA	By SIOS
ADSC	#1	3.5 ± 1.6	3.2 ± 1.6	175	118.9
	#2	2.8 ± 1.5	1.4 ± 0.26	169	127.8
	#3	1.7 ± 0.55	1.6 ± 0.56	136	—
	#4	3.8 ± 1.1	—	160	117.3

Figure 3 | ADSCs secrete 100–200 nm exosomes. (A) A phase-contrast transmission electron micrograph of purified ADSC #4-derived exosomes. Scale bar: 100 nm. (B) The exosome fractions and cell lysates of ADSCs #1 and #4 were analyzed by immunoblotting with antibodies against exosomal proteins CD63 and CD81 and cellular proteins cytochrome-c (Cyt-c) and actin (CD63 under nonreducing conditions). Equal amounts of protein from cell lysates or exosomes were used for each assay: 0.5 μg for CD63, 5 μg for CD81 and Cyt-c, and 1 μg for actin. (C, D) Size distribution of ADSC#1-derived exosomes as measured by nanoparticle tracking analysis (NTA) showed a peak at 175 nm (C), and scanning ion occlusion sensing (SIOS) showed a peak at 118.9 nm (D). (E) Yields and peak diameters of exosomes produced by ADSCs #1–4 are summarized. Protein amounts and particle numbers of harvested exosomes were determined by the Bradford method and NTA, respectively. Peak diameters were determined by NTA and SIOS. Data are the mean ± S.D. (n = 3–4).

exosomes were incorporated into N2a cells (Fig. 6B). Seven hr after exosome addition to N2a culture medium, some of the cells were already stained green. Furthermore, after 24 hr, most N2a cells were stained green, indicating that ADSC-derived exosomes were efficiently transferred into recipient N2a cells. Collectively, it was demonstrated that ADSCs transferred their exosomes to N2a cells, which may lead to the decrease in the intracellular Aβ42 level of N2a cells.

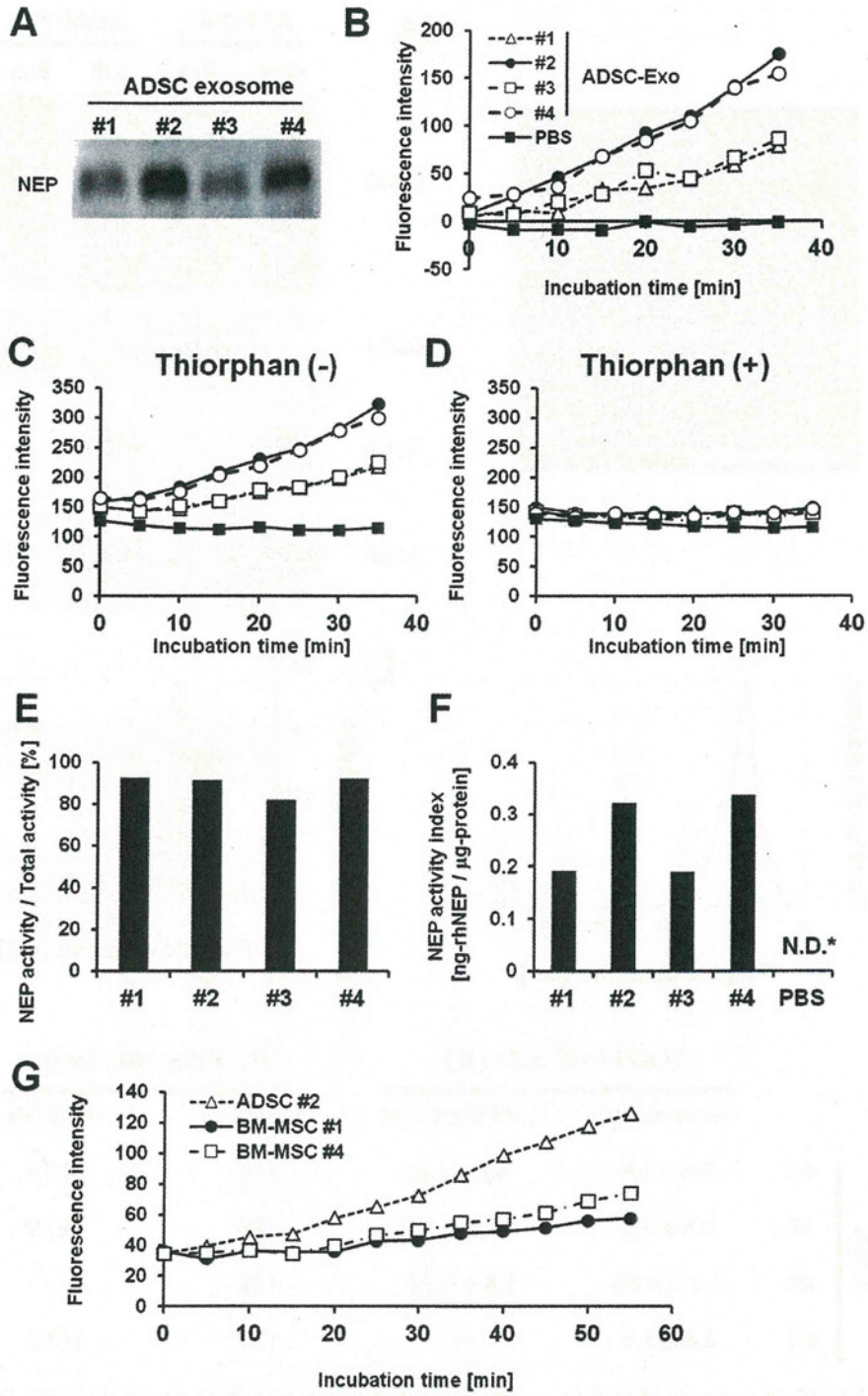

Figure 4 | ADSC-derived exosomes possess enzymatically active NEP. (A) Immunoblotting for NEP of exosomes isolated from ADSCs #1–4. (B–D) NEP enzyme activity assay for ADSC-derived exosomes (#1–4). NEP enzyme activity was measured using a fluorogenic peptide substrate, Mca-RPPGFSAFK(Dnp) and NEP inhibitor thiorphan. NEP specific activity (B) was calculated by subtracting the residual fluorescence intensity measured in the presence of thiorphan (D) from the total enzyme activity measured in the absence of thiorphan (C). Addition of thiorphan sharply reduced the enzyme activity of ADSC-derived exosomes (D). (E) NEP contribution ratio for ADSC-derived exosomes calculated as the percentage ratio of NEP-specific activity rate to total activity rate. (F) NEP-specific enzyme activity levels of exosome fractions of ADSCs #1–4 were estimated from a rhNEP standard curve (Fig. 4S) and are represented as the value ng-rhNEP/µg protein (termed as NEP activity index in the diagram). N.D. indicates "not determined".

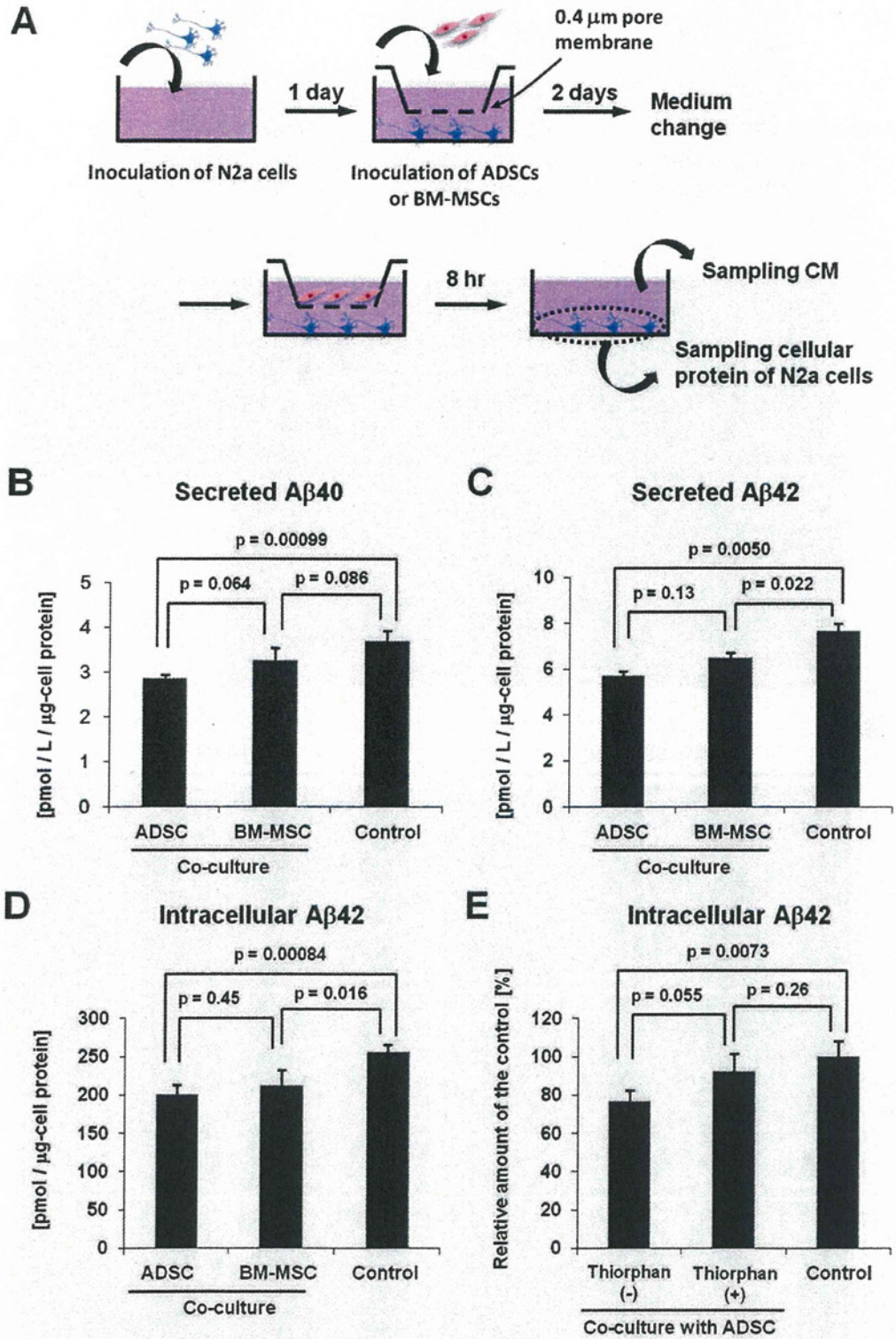

Figure 5 | ADSCs decrease both the extracellular and intracellular Aβ levels of N2a cells. (A) Schematic representation of the co-culture experiments of N2a cells with ADSCs or BM-MSCs using cell culture inserts. Secreted Aβ40 (B) and Aβ42 (C) levels were measured using the collected CM in the bottom chambers by ELISA. Each value was normalized to the protein content of N2a cell lysates. Data are the mean ± S.D. (n = 4). (D) Intracellular Aβ42 levels were measured using the N2a cell lysates by ELISA. Each value was normalized to the protein content of N2a cell lysates. (E) Intracellular Aβ42 levels were compared in co-cultures of ADSCs and N2a cells in the presence and absence of thiorphan. Each value is shown as the relative level to the control. Data are the mean ± S.D. (n = 4).